Recent advances in Ni-mediated ethylene enchainment: N-donor ligand effects on catalytic activity, thermal stability and oligo-/polymer structure

Zheng Wang [a,b,c], Qingbin Liu,*[,c] Gregory A. Solan,*[,a,d] Wen-Hua Sun *[,a,b,e]

A special issue in honor of Prof. Pierre Braunstein

[a] Key Laboratory of Engineering Plastics and Beijing National Laboratory for Molecular Science, Institute of Chemistry, Chinese Academy of Sciences, Beijing 100190, China

[b] CAS Research/Education Center for Excellence in Molecular Sciences, University of Chinese Academy of Sciences, Beijing 100049, China

[c] College of Chemistry and Material Science, Hebei Normal University, Shijiazhuang 050024, China

[d] Department of Chemistry, University of Leicester, University Road, Leicester LE1 7RH, UK

[e] State Key Laboratory for Oxo Synthesis and Selective Oxidation, Lanzhou Institute of Chemical Physics, Chinese Academy of Sciences, Lanzhou 730000, China

Contents

ABSTRACT

Homogeneous nickel catalysts have a considerable track record for mediating ethylene enchainment in the form of oligomerization and more recently polymerization. Within the polymerization arena, high molecular weight materials incorporating various degrees of

branching, anywhere from linear to moderately branched through to hyperbranched, highlight the versatility of this type of catalyst. This review focuses on recent progress related to structural modifications made to the pre-catalyst, and in particular to the *N*-ligand manifold, and how these changes impact on thermal stability and activity of the catalyst as well as the microstructural properties of the polyethylene and the distribution of the oligomeric fractions. In addition to ongoing process development directed towards commodity-type polyolefinic materials, the emergence of nickel catalysts that can form elastomeric-type materials from a single ethylene feed, without the addition of a high-cost α-olefin such as 1-hexene or 1-octene, offers considerable opportunities for future commercial applications.

Keywords: Nickel catalyst; Ethylene; Polymerization; Oligomerization; N-donor ligand; Catalytic activity; Thermal stability; Polyethylene microstructure; Branching.

Graphic Abstract

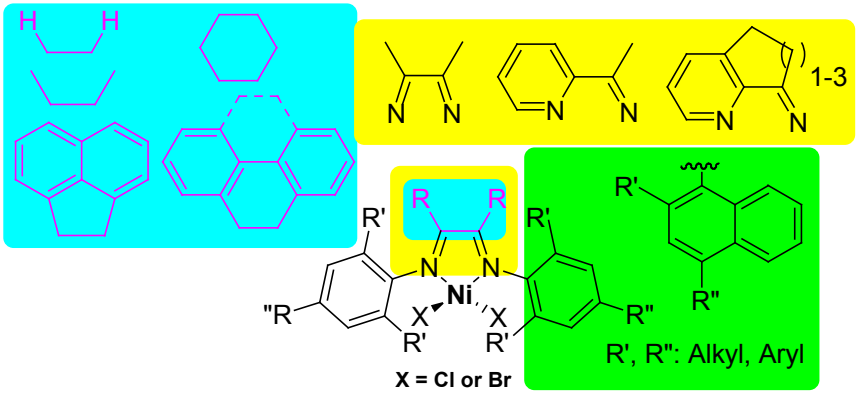

1. Introduction

Among the most important materials manufactured by the petrochemical industry are polyolefins, with polyethylene accounting for the largest sector of the market. Linear α-olefins constitute another important class of material which can be used as co-monomers in the production of polyolefins and as precursors to detergents, plasticizers and lubricants [1]. A wide variety of catalysts can promote the enchainment of an olefin to give a polyolefin (and/or an α-olefin) including complexes based on late transition

metals. Most notably, the α-diimine-nickel complexes first disclosed by Brookhart more than two decades ago, are highly active catalysts for the formation of high molecular weight polyethylene [2]. Furthermore, this type of catalyst produces polymers incorporating a range of branching contents and also exhibits good tolerance towards functional groups/polar monomers [3-12]. Subsequently, Brookhart [13] and Gibson [14] independently extended the range of polymerization-active late transition metals to include iron and cobalt. Collectively, these discoveries have help create a new era in catalytic olefin polymerization that continues apace to this day. Numerous review articles have highlighted the progress in late transition metal pre-catalyst development and its influence on the resulting polyolefinic products [3-5,15-18]. In addition a range of feature articles and book chapters have also focused on iron- and cobalt-based systems [19-23]. However, despite recent key developments, only few reviews have been dedicated to the subject of nickel-based homogeneous technology [24-26].

As regards N^N-type α-diimine-nickel pre-catalysts, the alkyl substitution pattern of the N-aryl groups and ligand backbone exerts a significant influence on the polymerization activities and polymer microstructures [24-28]. Nevertheless, this modulation of the steric/electronic properties of these groups still tends to afford high molecular weight materials. By contrast, pyridinylimine-based N^N-nickel pre-catalysts, in the main, promote the conversion of ethylene to α-olefins with the ligand structure, substitution effects and process conditions playing an important role on the catalytic activity and product distribution [24,25,29]. Elsewhere, Braunstein and co-workers have made significant contributions in the field of catalytic ethylene oligomerization [30-45] and, in particular, with regard to the preparation and application of P^N [30-32,34,36], P^P [38,40], N^P^N [37] and SHOP-type [35,38] nickel complexes for olefin oligomerization. In general, however, it still remains difficult to achieve performance characteristics that can compete with industrial catalysts. Nonetheless, studies of this type focusing on the effects of the fine structure of the nickel complex on the catalytic activity

and the selectivity for α-olefins have been fundamental to the design and development of high carbon α-olefin catalysts that have shown industrial promise.

Over the years our group has been interested in further exploring the scope, versatility and thermal stability of well-defined nickel(II) complexes as pre-catalysts for ethylene polymerization (and oligomerization). Besides being a source of academic interest, these new catalytic systems and their resulting polyolefinic products have displayed genuine potential for industrial applications. Herein, we collect together some of the more recent results within the field with the main emphasis being placed on the types of ancillary multidentate nitrogen donor ligand deployed at the metal center and how their fine tuning can influence the activity, selectivity (*e.g.*, polymer versus oligomer or carbon content of α-olefin) and thermal stability of the catalyst along with the microstructural properties of the oligo-/polymer itself. We hope our collected findings will illustrate the value of the research and furthermore will encourage other researchers to become involved in the challenges ahead.

2. Nickel pre-catalysts bearing N^N-chelating ligands

Since the seminal discovery that α-diimine-nickel complexes can efficiently catalyze the polymerization of ethylene [2], the synthesis of structurally related N^N-nickel-based complexes has emerged as a hot topic in not only catalytic olefin polymerization but also coordination chemistry in general [24-26]. In this section we focus our discussion on developments involving the archetypal α-diimine and pyridinylimine N^N-ligand systems as well as some closely related variants. Synthesis of these imine-based ligands generally makes use of straightforward condensation strategies involving the acid-catalyzed reaction of a carbonyl (ketone or aldehyde) precursor with an aniline [25]. Complexation can be readily achieved by treating the neutral N^N ligand with a suitable nickel(II) salt.

2.1. α-Diimine and related nickel catalysts

< **Figure 1**>

In 1995, Brookhart *et al.* reported the first examples of α-diimine-nickel(II) halide complexes, **1a-c**, that could be employed as pre-catalysts for ethylene polymerization (Fig. 1) [2]. In the presence of ethylene and with MAO as co-catalyst, **1a-c** were able to produce highly linear through to moderately branched polyethylene. Moreover, **1a-c** exhibited extremely high activities comparable to those of metallocene catalysts. For example, **1a** (R^1 = R^2 = *i*-Pr)/MAO, exhibited a turnover frequency of 3.9 × 10^5 h^{-1} (corresponding to 1.1 × 10^7 g(PE) mol^{-1}(Ni) h^{-1}) for ethylene polymerization [2]. Subsequently, a series of skeletal modifications to the α-diimine framework were introduced and structure-activity correlations evaluated [24-26]. In 2000, the Brookhart group reported the catalytic performance of the α-diimine-nickel complexes, **1c-e**, which on activation with MMAO exhibited high activities for ethylene polymerization (Fig. 1) [46]. In general, as the steric bulk and number of *ortho*-substituents increased, the polymer molecular weights, turnover frequencies and branching contents of the polyethylenes all simultaneously increased. Varying the backbones of the α-diimine can have a significant effect on the polymer microstructure and catalyst activity. All three nickel complexes, **1c-e** (containing the same bulky N-2,6-diisopropylphenyl groups), were very active polymerization catalysts with **1c** showing the highest turnover frequency. However, when compared with **1c** and **1d**, **1e** produced polyethylene with a higher molecular weight and a higher degree of branching. An additional effect of the alkyl-substituted backbone of the ligand is that the molecular weight distributions of the polyethylenes formed are less than those produced by the planar acenaphthene systems [46]. The mechanism of polymerization catalyzed by nickel complexes bearing α-diimine ligands is generally considered to be based on an active species comprising a cationic nickel-alkyl/hydride [47,48]; chain-walking (β-H elimination/reinsertion) during the chain propagation step are the principal reasons for the formation of branched

polyethylene [49].

< **Figure 2**>

With a view to improving the thermal stability of the α-diimine nickel catalysts, the Wu group investigated the polymerization behavior displayed by **2a**-**2c**, in which a set of systematic modifications were made to the α-diimine ligand skeleton (Fig. 2) [50,51]. In the presence of MAO, all these nickel complexes were active for ethylene polymerization. The bulky backbone-containing **2a** and **2b** revealed significantly higher thermal stability and produced higher molecular weight polyethylene as compared with the acenaphthene-containing **1c** (Fig. 1) [46,50]. In the presence of MMAO or Et_2AlCl, **2c** ($R^1 = R^2 = i$-Pr, $R^3 = H$) can polymerize ethylene in a living fashion over a period of 120 minutes at room temperature or above and produce narrowly-dispersed polyethylene (PDI < 1.10) with high molecular weight [51].

The Rieger group has investigated use of the α-diimine-nickel salts, **3a**, **3b** and **4**, for the gas phase polymerization of ethylene (Fig. 3) [52]. These catalysts showed moderate to high activities and produced polyethylene ranging from LLDPE to HDPE; the former PE grade being notably generated without the need for the addition of an α-olefin co-monomer. On comparison **3a** with **3b**, **3a** affords material of lower molecular weight containing terminal and internal double bonds while **3b** gives high molecular weight polyethylene [52].

< **Figure 3**>

The Li group has investigated the ethylene polymerization capability of **5a** and **5b** bearing 9,10-phenanthrenequinone-based α-diimine ligands (Fig. 3) [53]. In the presence of MAO, both complexes exhibited high productivities and generated high molecular weight polyethylene ($1.26\text{-}2.14 \times 10^6$ g mol^{-1}). Moreover, the molecular weight of the polymer formed by **5a** is much higher than that obtained by the prototypical α-diimine nickel complexes, **1a-c** (Fig. 1). For example, using **5a** at 0 ºC the molecular weight falls between 2.6 and 12.7×10^5 g mol^{-1}, while for **1a**/**1b** ($R^1 = R^2 =$ Me, R = H or Me [2]), at

the same temperature, it is 4.3-17.0 × 10^4 g mol^{-1}. In the same way, at 30 ºC the molecular weight lies between 2.2 and 3.4 × 10^5 g mol^{-1} for **5a**, while for **1c** (R^1 = R^2 = Me [46]) at 35 ºC, it is 1.43 × 10^4 g mol^{-1}. In addition, **5b** produced polyethylene with lower molecular weight when compared to that obtained by **5a** [53].

Our group has also explored the ethylene polymerization performance of the nickel dihalides (X = Cl, Br), **6**, bearing the 4,5-bis(arylimino)pyrenylidene N^N-ligands (Fig. 3) [54]. On activation with a range of co-catalysts including MAO, EASC and MMAO, **6** exhibited high activities up to 4.42 × 10^6 g(PE) mol^{-1} (Ni) h^{-1} and produced polyethylenes with a high degree of branching (up to 130 branched per 1000 carbons) and narrow molecular weight distributions. When MAO was used, the catalytic activity decreases in the order: **6** (Ar = 4-methyl-2,6-diethylphenyl) > **6** (Ar = mesityl) > **6** (Ar = 2,6-dimethylphenyl) for the bromides and **6** (Ar = mesityl) > **6** (Ar = 2,6-dimethylphenyl) for the chlorides. The reaction parameters, including the Al/Ni molar ratio, the reaction temperature and time, have a significant influence on the catalytic activity and properties of the so-formed polyethylene. The polyethylene products were shown to be highly branched [54].

The thermal instability of α-diimine-nickel catalysts has often been levelled as a drawback of these systems that has likely prevented their use in industrial applications [16,19-21,26]. With the aim of improving the thermal stability, many research groups have been concerned with exploring features within the diimine skeleton that could improve it [24-26]. Brookhart *et al.* reported that the N-C bond of the N-aryl group undergoes axial rotation at elevated temperature with the result that the N-aryl group, which is perpendicular to the N_2Ni plane at lower temperature, adopts a parallel mode at higher temperature [55]. Under such conditions, the hydrogen atoms belonging to the 2,6-substituted alkyl groups are in close proximity to the central metal resulting in agostic interactions with the metal ion, which ultimately leads to the deactivation of the catalytic system. On the basis of this theory, several research teams have been concerned with

designing new ligands sets that are capable of preventing this axial rotation of the N-aryl group.

Guan *et al.* have investigated the ethylene polymerization behavior of the cyclophane-containing α-diimine nickel catalysts **7a** and **7b** (Fig. 4) [56,57]. Complex **7a** exhibits excellent activity for ethylene polymerization with a productivity of 4.2×10^7 g(PE) mol^{-1} (Ni) h^{-1} [56]. Due to the rigid structure of the cyclophane framework, the probability of the occurrence of a meta-junction effect between the central metal of the complex and the hydrogen atom of the substituted N-aryl group is reduced. In addition, the active center in **7a** and **7b** is located at the heart of the macrocycle, allowing only ethylene insertion and ethylene chain growth to occur in both directions, thus achieving the desired protection of the active center. Notably even at 90 ºC, the catalytic activity remained high (TOF = 1.071×10^6 h^{-1} for **7a**) (Fig. 4) [56]. Although the polymer productivity of **7b** is lower than the non-fluorinated analogue **7a**, **7b** exhibits increased thermal stability when compared with **7a**. Indeed, **7b** remained active after 70 minutes at 105 ºC with scarcely any loss in polymerization activity. In addition, the polymer formed displayed a bimodal molecular weight distribution, consisting of a high molecular weight major fraction ($M_n \approx 10^5$ g mol^{-1}) and a minor proportion based on ultrahigh molecular weight polymer ($M_n > 10^6$ $gmol^{-1}$) [57]. The same group also synthesized the alkyl-bridged macrocyclic-containing **8** (Fig. 4) and showed this pre-catalyst to possess a lower activity (TON < 400) for ethylene polymerization [58]. In view of this result, Guan *et al.* modified **8** to generate the semi-cyclic complexes **9** and **10** (Fig. 4) [59]. In the presence of $AlMe_2Cl$, **9** showed high activity (TON > 5.88×10^5 h^{-1}) for ethylene polymerization and produced polyethylene with high molecular weight and relatively narrow polydispersity (PDI = 2.2). In sharp contrast, **10** containing a non-donating phenyl group, only afforded low molecular weight oligomers with broad polydispersities (PDI ≥ 5.6) when using either MAO, $AlMe_3$ or $AlMe_2Cl$ as the activator. The axial donating pyridine group in catalyst **9** can thus prevent chain transfer. The absence of such axial interactions in **10** results in

high susceptibility to chain transfer from the open bottom face, leading to low molecular weight oligomers [59].

< **Figure 4**>

Furthermore, the axial pyridine unit in **9** reversibly interacts with the metal center, providing electrons for the active 14 valence electron metal center in the axial direction to stabilize it, suppressing β-H elimination [47-49], thereby preventing the occurrence of a chain transfer reaction and achieving temporary protection to the catalytic intermediates. Hence, the rate of chain transfer is suppressed resulting in high molecular weight linear polyethylene.

< **Figure 5**>

Based on steric considerations, our group has also made some progress with improving the thermal stability of α-diimine-nickel catalysts (Figs. 5-7) [24-26]. By introducing benzhydryl [$CH(Ph)_2$] or difluorobenzhydryl [$CH(p\text{-}FPh)_2$] as the substituents on the N-aryl groups, the unsymmetrical **11** and **12** as well as symmetrical **13** can be accessed (Fig. 5) [60-73]. Complexes **11-13** all showed high catalytic activity and good thermal stability for ethylene polymerization [60-62]. With regard to **11**, activation with either MAO or MMAO, generated a high activity catalyst producing polyethylene of high molecular weight and displaying a high degree of branching [60]. Notably, the co-catalyst employed can affect the properties of the polyethylene obtained. For example, treating **11** with MAO, afforded polyethylene exhibiting bimodal characteristics, whereas that resulting from the use of MMAO showed unimodal characteristics [60]. Upon activation with either MAO or MMAO, difluorobenzhydryl substituted-**12** exhibited higher catalytic activity (up to 10^7 g(PE) mol^{-1}(Ni) h^{-1}) than that of **11** [61] and afforded highly branched polyethylene with a bimodal distribution. Upon activation with Et_2AlCl, **13**, based on the remotely substituted *para*-benzhydryl groups, exhibited high activity (10^6 g(PE) mol^{-1}(Ni) h^{-1}) [62] and produced polyethylenes with low levels of branches. In general, the polyethylenes obtained using **11-13** display high molecular weights (10^5 g mol^{-1} or more)

and narrow molecular weight distributions (PDI: 2 to 4). For **13**, their catalytic activities decrease in the order, **13a** > **13b** > **13c** >> **13d** > **13e**; highlighting the negative influence of bulky substituents on the activity. On the other hand, the molecular weights of the polyethylenes increase in the order, **13a** < **13b** < **13c** << **13d** < **13e**, which suggests that bulky substituents hinder the chain migration and the termination process related to it. The *ortho*-substituted benzhydryl-containing **13d** and **13e** display better thermal stability than *ortho*-substituted Me/Et/i-Pr **13a-c**, underlining the effect steric hindrance has on thermal stability of the catalyst [62].

< **Figure 6**>

Complexes **14a-d** and **15a-c**, each containing one N-aryl group appended with various benzhydryl substitution patterns, show outstanding catalytic activity and form polyethylene exhibiting a high degree of branching (Fig. 6) [63-68]. When the *para*-R group is Me (**14a**), activation with either Et_2AlCl or MAO, led to an exceptionally active catalyst (up to 1.1×10^7 g(PE) mol^{-1}(Ni) h^{-1}) producing highly branched polyethylene [63]. In the same way, when the *para*-R group is Cl (**14b**), using MAO as co-catalyst, **14b** also showed exceptionally high activities (up to 1.48×10^7 g(PE) mol^{-1}(Ni) h^{-1}) affording branched polyethylenes of high molecular weight (M_w up to 10^6 g mol^{-1}) [64]. Likewise, when *para*-R is F (**14c**), **14c**/MAO was highly active (1.49×10^7 g(PE) mol^{-1} (Ni) h^{-1}) producing similarly branched polyethylenes with molecular weights of up to 1.62×10^6 g mol^{-1} and narrow polydispersities [65]. Incorporation of a *para*-nitro substituent (**14d**), and activation with either Et_2AlCl or EASC, again provided high activity; importantly the resultant polyethylenes possessed ultra-high molecular weights in the range of 10^6 g mol^{-1} with narrow molecular weight distributions [66].

For the series based on **15**, incorporating a 2,4- or 2,4,6-substitution pattern for the benzhydryl groups, high activity is retained and good thermal stability is a feature of the ethylene catalysis (Fig. 6). When the *ortho*-R group is Me (**15a**), **15a**/MMAO delivers high activities of up to 8.95×10^6 g(PE) mol^{-1} (Ni) h^{-1}, affording highly branched polyethylene

products [67]. When the *ortho*-R group is Cl (**15b**), **15b** in the presence of relatively low amounts of EASC, also exhibits high activities of up to 1.09×10^7 g(PE) mol^{-1} (Ni) h^{-1} producing branched polyethylenes. Significantly, even at 80 ºC, both these systems showed good thermal stability by maintaining high activity at this temperature (up to 3.76×10^6 g(PE) mol^{-1} (Ni) h^{-1}) [68]. When the *ortho*-R group is $CH(Ph)_2$ (**15c**), high activity is again apparent (up to 1.07×10^7 g(PE) mol^{-1} (Ni) h^{-1}) with the catalyst showing good thermal stability even at 90 ºC (2.97×10^6 g(PE) mol^{-1} (Ni) h^{-1}), producing hyperbranched polyethylenes. Significantly these polymeric materials possess good elastomeric recovery and high elongation at break as determined by dynamic mechanical analysis and stress-strain testing; we view these polymers to have great potential as alternative materials to thermoplastic elastomers [69].

On activation with either MAO or Et_2AlCl, the (2-benzhydrylnaphthyl)imino-modified nickel complexes, **16**, showed moderate activities toward ethylene polymerization (Fig. 7) [70]. The resulting polyethylenes revealed high molecular weights and branching contents lower than that observed using the diiminoacenaphthene-nickel derivatives **14a**, **14b** and **15a** (Fig. 6) [63,64,67].

< **Figure 7**>

With either MAO or Et_2AlCl as co-catalysts, **17a** and **17b**, bearing sterically bulky diiminoacenaphthene ligands, behaved as polymerization catalysts with very high activities, up to 10^7 g(PE) mol^{-1} (Ni) h^{-1} (Fig. 7) [71, 72]. Even at 80 ºC, a common industrial operating temperature, these catalytic systems still maintained remarkably high activities of up to 4.87×10^6 g (PE) mol^{-1}(Ni) h^{-1} [71, 72]. More importantly, the polymer obtained using **17b** (incorporating the 2,6-substituted difluorobenzhydryl groups) was highly branched, narrowly dispersed with a molecular weight of 10^5 g mol^{-1}; properties consistent with an elastomeric material [73]. Notably such materials are of high demand in industrial applications [72]. Likewise, **18a** and **18b**, bearing difluorobenzhydryl groups at the 2-position of either one (**18a**) or both N-aryl groups (**18b**), displayed high catalytic

activities up to 10^6 g(PE) mol^{-1} (Ni) h^{-1}, in the presence of either MAO and EASC (Fig. 7) [74]. Pre-catalyst **18b** notably exhibited good thermal stability at temperatures in the range 60 – 80 °C, generating polyethylenes with high molecular weight of up to 10^6 g mol^{-1} [74].

Complexes **19** [75], bearing a 4-fluoro-2,6-bis(fluorobenzyhdryl)phenyl unit as one of the two N-aryl groups on the diaryliminoacenaphthene, gave on activation with EASC at relatively low Al/Ni ratios (ca. 600 equiv.), extremely high catalytic activities of up to 2.20 × 10^7 g(PE) mol^{-1}(Ni) h^{-1} at 30 °C (Fig. 8). The bromide pre-catalysts showed higher activities than their chloride analogues, while the chloride pre-catalysts required less co-catalyst [75]. In comparison with unsymmetrical **17b**, **18a** and **18b** (Fig. 7) [72,74,75], **19** exhibits higher activities which has been ascribed to the electron withdrawing properties of the *para*-fluorides and their effect on the net charge of the active catalyst [75].

< **Figure 8**>

We have also investigated the effect of difluorobenzhydryl-substitution on N-naphthyl-containing unsymmetrical complexes **20** (Fig. 8) [76]. In the presence of Et_2AlCl, **20** were highly active, generating polyethylenes with high molecular weights ranging from 0.86 – 5.58 × 10^5 g mol^{-1} and showing narrow polydispersities (1.22–1.99). In an attempt to balance more effectively good thermal stability with high activity we have investigated pre-catalysts containing *ortho*-substituted difluorobenzhydryl-substitution on both (**21**) or just one of the N-aryl groups (**22**) of the diaryliminoacenaphthene (Fig. 8) [77]. Upon activation with either MAO or Et_2AlCl, **21** and **22** displayed outstanding activity toward ethylene polymerization (up to 1.02 × 10^7 g(PE) mol^{-1}(Ni) h^{-1}). It is worthy of note that **21** bearing equivalent difluorobenzhydryl-substituted N-aryl groups was able in the presence of Et_2AlCl to successfully couple high activity with exceptional thermal stability with an activity up to 1.12 × 10^6 g(PE) mol^{-1} (Ni) h^{-1} generating high molecular weight (up to 10^5 g mol^{-1}) branched polyethylenes at temperatures as high as 100 °C [77].

As is evident from the above, fine tuning of the structural features of the pre-catalyst can not only affect the activity and thermal stability of the catalyst but it can also influence the microstructures and properties of the resulting polyethylenes. Tables 1 and 2 collect together some reported polymer data for a series of polyethylenes obtained under comparable polymerization conditions, using a set of structurally distinct unsymmetrical diiminoacenaphthene-nickel pre-catalysts. With MAO as activator and the run temperature at 30 °C, pre-catalysts **14c**, **17b**, **22**, **18a** and **16** produced polyethylenes exhibiting a range of different branching and melting temperatures (Table 1). For example **14c** and **17b**, incorporating 2,6-bis(benzhydryl)phenyl-imino groups, resulted in highly branched (> 113 per 1000 carbons) polyethylenes with low T_m's (< 60 °C) [65, 72]. Conversely, **22** incorporating a 2,4-bis(*p*-fluorobenzhydryl)aryl-imino groups gave polyethylenes with higher T_m values (> 99 °C) and lower levels of branching (~44 per 1000 carbons) [77]. For **18a** and **16**, incorporating 2-substituted benzhydryl groups, the polymeric materials displayed the highest T_m's (> 111 °C) and lowest branching contents (≤ 27 per 1000 carbons) of this series [70,74]. The temperature at which the polymerization run is conducted also plays a key role as to the branching content of the polymers: typically higher run temperatures lead to materials displaying lower melting temperatures and increased degrees of branching. For example, using **16**/MAO at 60 °C produced polyethylene with a T_m of 102 °C as opposed the 124 °C at 30 °C, while the branching content was 42 per 1000 carbons at 60 °C and 17 per 1000 carbons at 30 °C [70]. Similarly with **17b**/MAO at 50 °C, the polymer showed 140 per 1000 carbons, while at 30 °C the number lowers to 113 per 1000 carbons at [72].

< **Table 1**>

Similar structural and temperature effects on the polymeric properties are seen with different activators. For instance with Et_2AlCl as activator and the run temperature at 30 °C (Table 2), the most sterically bulky **15c** and **17b**, bearing 2,6-bis(benzhydryl)aryl-imino groups, again resulted in polyethylenes with low T_m's (<

61 ºC) and high branching contents (≥ 95 per 1000 carbons) [69, 72]. Using **22**, containing 2,4-bis(*p*-fluorobenzhydryl)phenyl-imino groups, produced polyethylenes with higher T_m's (> 100 ºC) and lower levels of branches (~38 per 1000 carbons) [77]. In the case of **16**, containing a 2-benzhydrylnaphthyl-imino group, gave polyethylenes with the highest T_m (> 130 ºC) and lowest number of branches (~24 per 1000 carbons) at this temperature [70]. Increasing the temperature to 50 ºC, **17b** gave polyethylenes with the lowest T_m (< 44 ºC) of this series of pre-catalysts and displaying the most branches (~ 150 per 1000 carbons) [72].

< **Table 2**>

Other research groups have also reported the benzhydryl-modified symmetrical α-diimine nickel complexes. For example, the Long group has investigated the use of synthetically simpler dibenzhydryl as the *ortho* N-aryl substituents on pre-catalysts **23** and **24** for ethylene polymerization (Fig. 9) [78,79]. These nickel complexes have been shown to display remarkable thermal stability during the polymerization runs. In the presence of MAO, **23** showed high catalytic activity in the temperature range 80 − 100 ºC reaching 2.12 × 10^6 g(PE) mol^{-1}(Ni) h^{-1} at 100 °C. The polyethylene produced showed a well-defined molecular weight distribution ($M_w/M_n \leq 1.31$), with high molecular weight ($M_n > 6\times10^5$ g mol^{-1}), and was moderately branched (63−75 branches per 1000 carbons) [78]. As with **23**, **24** displayed impressive thermal stability up to 90 °C. More significantly, **24** exhibited TOFs 1.4 times greater than that seen for **23**, producing polyethylene with melting temperatures increased by *ca.* 20 °C, and yielding fewer branches per 1000 carbons than polymers made with catalysts bearing alkyl-substituted backbones [79].

< **Figure 9**>

Rishina and co-workers have investigated the use of fluoro- (**25a**) and trifluoro-methylphenyl-containing (**25b** and **25c**) α-diimine nickel complexes as catalyst precursors in oligomerization reactions of ethylene and propylene (Fig. 9) [80]. Using **25a-c** in combination with a mixture of $AlEt_2Cl$ (or $Al_2Et_3Cl_3$) and PPh_3, ethylene

enchainment at 30 °C occurred yielding mixtures of waxy and liquid oligomers (the oligomerization degree 6–9) containing 14-20 mol% of methyl branches, 4-6 mol% of ethyl branches and a small number of longer chain branches. Using propylene as the monomer at temperatures between 30–70 ^{o}C, these catalysts produced mixtures of very light oligomers (mostly dimers). Complex **25b** produced an active species that exhibits no regioselectivity, whereas using **25a** some preference for primary insertion was observed [80].

< **Figure 10**>

2.2 Pyridinylimine and related nickel catalysts

As with the α-diimine-nickel-based systems discussed above, pyridinylimine- (and quinolinylimine) nickel(II) complexes have also been the subject of many reports in recent years. In this section we review the impact that this structural variation has on the performance of the resulting nickel catalysts in ethylene oligo-/polymerization [24-26].

< **Figure 11**>

A series of pyridinylimine-nickel catalysts based on sterically hindered benzhydryl-containing pyridinylimine ligands have been developed in our laboratory (**26** in Fig. 11) [81]. In the presence of either MAO or EASC, **26** exhibited high activities (up to 10^7 g mol^{-1} (Ni) h^{-1}) in ethylene polymerization, producing moderately branched polyethylene of low molecule weight (~2.0×10^3 g mol^{-1}) and narrow polydispersity (PDI ≤ 2.52) [80]. Recently we increased the steric bulk of **26** by the introduction of R = *t*-butyl with the result that the catalytic activities remained high as 10^6 g mol^{-1} (Ni) h^{-1}, but the products were now short-chain oligomers [82].

Elsewhere Wu *et al.* reported that a set of related pyridinylamine-nickel complexes, **27**, containing a various skeletal substitutions, are active pre-catalysts for ethylene polymerization (Fig. 11) [83, 84]. A di-block copolymer polyethylene-poly (1-hexene) can also be synthesized using **27b** (R^1 = *i*-Pr, R^2 = H) in the presence of MAO [83].

Notably, the introduction of bulky aryl groups onto the pyridine moiety of the N^N-ligand led to a significant decrease in the activity and molecular weight of the polyethylene, whereas an increase in the steric bulk of the substituents on the amine-carbon caused an increase in both the polymerization activity and molecular weight of the polymer. With respect to the N-aryl group, increasing the steric hindrance results in decreasing the activity and affords a higher molecular weight polyethylene with a narrower polydispersity. By contrast, introduction of an electron-donating group on the N-aryl group leads to enhanced activity and the formation of a high molecular weight polyethylene [84].

< **Figure 12**>

The introduction of benzhydryl-substituted N-naphthyl groups into the pyridinylimine framework by synthesizing nickel(II) complexes, **28a** and **28b** has been disclosed by ourselves (Fig. 12) [85,86]. When activated with Et_2AlCl, **28a** performed with high activity (up to 1.22×10^7 g(PE) mol^{-1}(Ni) h^{-1}), generating polyethylene with high levels of branching, low molecular weight and narrow polydispersity [85]. Upon activation with either MAO or MMAO, **28b** exhibited even higher activity (up to 2.02×10^7 g (PE) mol^{-1}(Ni) h^{-1}) forming branched polyethylene of low molecular weight and narrow polydispersity (Fig. 12) [86].

< **Figure 13**>

Bryliakov and Antonov reported two families of pyridinylimine-nickel complexes **29** and **30** bearing electron-withdrawing groups in the ligand core for ethylene oligomerization and polymerization (Fig. 13) [87]. On treatment with MAO, **29** and **30** showed high activity (up to 9.6×10^6 g mol^{-1}(Ni) h^{-1} bar^{-1} for ethylene oligomerization and 6.6×10^6 g(PE) mol^{-1} (Ni) $h^{-1}bar^{-1}$ for ethylene polymerization) affording highly branched low molecular weight polyethylene with 86-229 branches/1000C's or ethylene oligomers consisting of predominantly butenes and hexenes, respectively [87].

< **Figure 14**>

The Darkwa group investigated the ethylene oligomerization capacity of discrete **31a** and **31b** along with silica-supported **32** with a view to studying the ease of separation of catalysts from the products in the catalytic process (Fig. 14) [88]. On activation with $EtAlCl_2$, all the complexes form active catalysts which dimerize ethylene to mainly butenes which subsequently undergo Friedel-Crafts alkylation of toluene (the solvent used for the ethylene reactions); leading to the formation of regioisomers of mono-, di- and tri-butyltoluenes. Significantly, **31a** and **31b** are the first examples of homogeneous nickel catalysts that can promote tandem ethylene oligomerization and Friedel-Crafts alkylation reactions to alkyltoluenes, an outcome also achievable when immobilized on a silica support (**32**). Although, the catalytic activity of the immobilized catalyst is lower than the homogeneous ones, **32** can perform these tandem reactions at higher temperature than the homogeneous counterparts, thereby offering a catalytic system that can withstand higher operating temperatures [88].

With an eye to developing new effective catalysts with enhanced catalyst stability, the Darkwa group has also investigated using the sterically bulky ferrocenyl group as a substituent for pyridinylpyrazolyl and pyrazolyl ligands for nickel(II) bromide complexes, **33a-e** (Fig. 15) [89]. Activation of complexes **33a-e** with $EtAlCl_2$ in chlorobenzene produced active species that catalyzed ethylene oligomerization. Oligomer analysis reveals the formation of butenes and then skips to C_6–C_{14} products and finally to C_{16}–C_{64} olefins; a non-Schulz–Flory distribution of products is apparent. Complexes **33a** (**33c**) and **33e** were the most active (1.776×10^6 g of ethylene oligomer mol^{-1} (Ni) h^{-1} and 1.989×10^6 g of ethylene oligomer mol^{-1} (Ni) h^{-1}, respectively) and, in toluene, produced isomers of butene and small amounts of butyltoluenes *via* Friedel–Crafts alkylation of toluene by the butenes [89].

< **Figure 15**>

Braunstein *et al.* have not only studied nickel complexes containing phosphorus donor ligands for the olefin oligomerization [30-40], but also nickel complexes, **34a-d**, bearing

two N^N-chelating pyridinyltriazole ligands (Fig. 15) [42]. On activation with $AlEtCl_2$, **34a-d** proved effective catalysts for the oligomerization of ethylene, showing moderate activities and turnover numbers.

< **Figure 16**>

Our team has also reported nickel complexes, **35**, bearing quinolinylimines for the oligomerization of ethylene (Fig. 16) [90, 91]. On activation with Et_2AlCl, **35** (R = Me) exhibited high activity for ethylene oligomerization (1.24-1.83 × 10^6 g mol^{-1}(Ni) h^{-1}) with good thermal stability at 60 °C under 10 atmospheres of ethylene. More interestingly, the addition of PPh_3 dramatically increased the catalytic activity (up to 1.72 × 10^7 g mol^{-1}(Ni) h^{-1}) of the system for ethylene oligomerization [90]. On activation with Et_2AlCl or EASC, **35** (X = Br) displayed high activity for the selective ethylene dimerization (0.89–3.29 × 10^6 g mol^{-1}(Ni) h^{-1}) at 20 °C under 10 atmospheres of ethylene, with α-C_4 as the main product [91]. The catalytic activities decreased on raising the reaction temperature. Further research efforts indicated that the ligand substituents present had a notable influence on the observed activities [91].

< **Figure 17**>

The application of pyridinyl-benzimidazoles and -benzoxazoles as the N^N-supporting ligand for nickel pre-catalysts in ethylene oligo-/polymerization is another area we have reported on (Fig. 17). For example, the pyridinylbenzimidazole-nickel complexes, **36a** and **36b**, on treatment with Et_2AlCl showed moderate to high ethylene oligomerization activity (5.87 × 10^5 g mol^{-1}(Ni) h^{-1} atm^{-1}) [92,93]. On the other hand, the pyridinylbenzoxazole-nickel complexes, **36c**, showed moderate to high catalytic activities (up to 4.15 × 10^5 g mol^{-1}(Ni) h^{-1} bar^{-1}) for ethylene oligomerization as well as the selective dimerization to give α-butene [93].

< **Figure 18**>

In recent years, our laboratory has developed an interest in studying the impact that fused cycloalkyl groups have on the catalytic performance of

N^N-pyridinylimine-nickel(II) catalysts [24]. For example, the 2-R-substituted 8-arylimino-5,6,7-tetrahydroquinoline-nickel complexes, **37a** (R = Ph) and **37b** (R = Cl), appended with less bulky N-aryl groups, on activation with $Et_3Al_2Cl_3$, convert ethylene into dimers (C_4) and trimers (C_6) with high catalytic activities (up to 9.5 $\times 10^6$ g mol^{-1}(Ni) h^{-1}) (Fig. 18) [94]. Good activity ($\leq 2.48 \times 10^5$ g mol^{-1}(Ni) h^{-1}) is also observed using more sterically hindered derivatives of **37a** (R = Ph) and **37b** (R = Cl) with MAO as the co-catalyst. However, in this case polymer is generated along with small amounts of C_4 with high α-olefin selectivity. These observations confirm that enhancing the steric bulk of the *ortho*-aryl-substituents (R^1) in **37a** and **37b** results in a higher ratio of solid polymer to oligomer [95]. For both **37a** and **37b**, the activities decreased in the order: 2,6-di(*i*Pr) > 2,6-di(Et) > 2,6-di(Me) and 2,6-di(Et)-4-Me > 2,4,6-tri(Me). Such phenomena are consistent with bulky alkyl substituents aiding the solubility of the pre-catalysts, which in-turn enhances activity [94,95]. For **37c** (R = Me) and **37d** (R = *i*-Pr) activation with EASC, resulted in high catalytic activities (up to 1.1 × 10^6 g mol^{-1}(Ni) h^{-1}) generating high selectivities for α-C_4; both catalysts showed good thermal stability at 80 ºC and 10 atmospheres of ethylene. In general, **37c** showed superior activities than that seen with **37d** [96]. Conversely, **37e** (R = H), when activated with either MAO or Et_2AlCl, formed branched polyethylene waxes with narrow polydispersity and high activity (up to 5.33 × 10^6 g(PE) mol^{-1} (Ni) h^{-1}) [97,98].

We have also investigated the ethylene polymerization capacity of the halide-bridged dinickel complexes, **38a-c**, using Et_2AlCl or MAO as the co-catalyst (Fig. 18) [99-101]. Upon activation with either MAO or Et_2AlCl, **38a** behaved as single-site catalysts for ethylene polymerization, forming polyethylene waxes with activities of up to 10^7 g(PE) mol^{-1} (Ni) h^{-1}. The molecular weights and distributions of the polyethylene waxes could be controlled by modifying the nature of substituents on the N-aryl groups in **38a** and the reaction conditions [99]. For **38b**, bearing either one or two bulky benzhydryl N-aryl substituents, treatment with either MAO or Et_2AlCl, again resulted in high activities (up

to 5.66 × 10^7g(PE) mol^{-1} (Ni) h^{-1}), producing wax-like products with narrow molecular weight distributions [100]. With **38c**, bearing nitro-substituted N-aryl groups, activation with EASC or MAO (required a smaller amount of co-catalyst) afforded a catalyst that showed high activities (up to 4.05 × 10^6 g(PE) mol^{-1} (Ni) h^{-1}) generating polyethylene without any evidence for oligomeric products [101]. Furthermore, it was observed that the presence of donor solvents such as tetrahydrofuran and pyridine, caused deactivation of the nickel pre-catalysts during the polymerization. All polymers obtained using **38c** are highly branched and potentially useful. Overall these results obtained for **37** and **38** imply that by constraining the N^N-pyridinylimine ligand, by incorporation of a cycloalkyl-fused pyridine unit, lead to an increase in the ethylene polymerization activity [94-101].

< **Scheme 1**>

In order to shed some light on the polymerization mechanism promoted by the imino-tetrahydroquinoline-nickel complex, **37e** (R^1 = R^2 = Me), Sun and Talsi used NMR and EPR spectroscopy to monitor its activation with AlR_2Cl (R = Me, Et) in toluene at -20 to 0 °C (Scheme 1) [102]. The findings revealed that activation of $LNiCl_2$ with $AlEt_2Cl$ affords the diamagnetic ion pair $[LNi^{II}Et]^+[AlEt_3Cl]^-$ (L = 2,4,6-trimethyl-(N-5,6,7-trihydroquinolin-8-ylidene)-phenylamine), whereas the use of $AlMe_2Cl$ as activator yields the paramagnetic ion pair with proposed structure $[LNi^{II}(\mu\text{-}R)_2AlMeCl]^+[AlMe_3Cl]^-$ (R = Cl or Me). Over time, both species convert to bis-ligated Ni(I) complexes with proposed structures $[L_2Ni^{I}]^+[A]^-$, where $[A]^-$ = $AlEt_3Cl^-$ or $AlMe_3Cl^-$, respectively. Monitoring of the ethylene reactivity reveals that $[LNi^{II}Et]^+[AlEt_3Cl]^-$ and $[LNi^{II}(\mu\text{-}R)_2AlMeCl]^+[AlMe_3Cl]^-$ are the closest precursors to the active species in the polymerization.

< **Figure 19**>

The effect of introducing one or more bulky benzhydryl substituents to the N-naphthyl group in 8-naphthylimino-5,6,7-tetrahydroquinoline-nickel pre-catalyst, **39**, has been studied (Fig. 19) [103]. On activation with either MMAO or Et_2AlCl, **39** exhibited high

activities (up to 8.29 × 10^6 g(PE) mol^{-1}(Ni) h^{-1} with MMAO, 6.66 ×10^6 g(PE) mol^{-1}(Ni) h^{-1} with Et_2AlCl), producing branched polyethylene with low molecular weights [103].

< **Figure 20**>

In a similar way, the addition of a bulky fluorenyl unit to the *para* and/or the *ortho* sites of the N-aryl group in 8-(arylimino)-5,6,7-trihydroquinoline in **40** has been explored (Fig. 20) [104]. Pre-catalysts **40d** and **40e** bearing a single fluorenyl substituent at the *ortho*-position gave polyethylenes with bimodal MWD's incorporating a high molecular weight tail. Further modulation of the polyethylene microstructure was achieved by the addition of Et_2Zn in terms of molecular weight, MWD and branching density. The Et_2Zn additive significantly changed the polymerization performance in **40d**/Et_2AlCl system; the resultant polyethylenes possessed higher molecular weights than observed in the absence of Et_2Zn [104].

< **Figure 21**>

With the intention of probing the influence of further ring fusion on the catalytic activity, we designed and prepared a series of 4-arylimino-1,2,3-trihydroacridyl-nickel(II) halide complexes, **41a** and **41b**, for evaluation as oligo-/polymerization pre-catalysts (Fig. 21) [105,106]. Using trimethylaluminum (TMA) as the activator, **41a** exhibited good activity (up to 8.36 × 10^5 g mol^{-1} (Ni) h^{-1}) for ethylene oligomerization generating oligomeric products ranging from butene (C_4) to hexadecene (C_{16}) [105]. The catalytic activities of **41b** were negatively affected by the propyl substituent on their cycloalkyl backbone when compared with the results obtained for unsubstituted **41a**. On activation with diethylaluminum chloride, **41b** exhibited moderate activity (up to 5.10 × 10^5 g mol^{-1}(Ni) h^{-1}) for ethylene oligomerization forming oligomeric products ranging from C_4 to C_{16} [106].

< **Figure 22**>

The impact of strain within the fused cycloalkyl ring of the N,N-ligand framework has been thoroughly investigated and shown to affect the catalytic performance of the nickel

pre-catalyst [107-111]. For example, the nickel complexes, **42**, chelated by a 9-aryliminocycloheptapyridine N^N ligand have been synthesized and assessed for their ability to promote ethylene enchainment (Fig. 22) [107,108]. On treatment with either MMAO or Et_2AlCl, all examples of **42** behaved as well-behaved single-site catalysts generating polyethylene with high activities (up to 7.80×10^6 g (PE) mol^{-1}(Ni) h^{-1}). The resultant polymers were highly branched with low molecular weights and narrow molecular weight distributions. Such properties are characteristic of polyethylene waxes that can have uses as additives to lubricants and pour-point depressants [107,108]. Complexes **42** showed comparable activities to that observed with cyclohexyl analogues **37** and **38** (Fig. 18), whilst exhibiting higher activities than that displayed by the parent pyridinylimine-nickel derivative **26** (Fig. 11). Hence, the ring-tension imposed by the presence of the cycloalkyl ring within the N^N ligand frame has enhancement effects on activity and influences the type oligo-/polymeric product [81].

With a view to targeting single-site active species we have found that fused cyclic ligand frameworks can provide rigid coordination environments around the nickel center, such as that seen in **37** and **38** (Fig. 18) [94-101]. However, one limitation of these imino-cycloalkylpyridines is their capacity to undergo imine–enamine tautomerization, which can lead to catalyst instability and multi-site behavior (Scheme 2).

<**Scheme 2**>

To inhibit the imine–enamine tautomerization, we have synthesized nickel complexes, **43a** and **43b**, bearing 8-arylimino-5,6-dihydro-7,7-dimethylquinoline derivatives and investigated their potential to perform as well-behaved catalysts for ethylene polymerization (Fig. 22) [109,110]. In the presence of either MAO or EASC, **43a** exhibited high activities (up to 6.48×10^5 g(PE) mol^{-1}(Ni) $h^{-1}atm^{-1}$) and produced polyethylene waxes with low molecular weights. The catalytic activities follow the order: [2,6-di(Me)] > [2,4,6-tri(Me)] > [2,6-di(Et)-4-Me] > [2,6-di(Et)]. Significantly, the polydispersities (1.7–2.0) obtained for the polyethylenes are narrow and are consistent

with a genuinely single-site active species for these catalysts [109]. With either MAO or Et_2AlCl as co-catalyst **43b**, bearing 8-(nitro/benzhydryl-arylimino)-7,7-dimethyl-5,6-dihydroquines as the chelating ligand, showed notable variations in the catalytic activities and polyethylene microstructure, owing to the interplay between electronic and steric effects [110]. Nickel pre-catalysts bearing the N^N-ligand with the electron-withdrawing substituent [$-NO_2$] tend to exhibit high activities in ethylene polymerization and generate both vinylene and vinyl groups within the polymer chains. On the other hand, bulky substituents [*e.g.*, $-CH(Ph)_2$] on the N-aryl group lead to low activities and vinylene groups present within the polyethylene chains. The differences in the catalytic activities of the nickel complexes, containing various halide ligands attached directly to the nickel atom [Cl or Br], could be rationalized by the trends in binding energies determined in the XPS study [110].

< **Figure 23**>

Our group have also synthesized a series of nickel complexes, **44** and **45**, bound by a new family of strained imino-cyclopenta[*b*]pyridines and explored their performance in ethylene polymerization (Fig. 23) [111]. On activation with either MAO or MMAO, **44** and **45** exhibited high activities towards ethylene polymerization with **44** (R^1 = Me) the most active (5.02×10^6 g (PE) mol^{-1} (Ni) h^{-1} at 20 °C); rapid regeneration of the active species (3096 – 5478 h^{-1} at 20 °C) is a feature of their catalytic performance. A detailed microstructural analysis of the polyethylenes revealed the presence of vinyl and higher levels of internal vinylene groups indicative of high rates of chain isomerization, *e.g.*, the ratio of (-CH=CH-) to (H_2C=CH-) groups is 2.2 : 1 using **44** (R^1 = Me)/MAO at 60 °C [111].

3. Nickel pre-catalysts bearing N^N^N-chelating ligands

While the application of N^N-nickel complexes in olefin oligo-/polymerization has led the way, there have also been a relatively large number of studies conducted using

tridentate N^N^N-systems [24, 26]. In general, however, the catalytic activities of these tridentate catalysts tend to be lower than those displayed by their bidentate analogues. Nevertheless, much promising work in the area has been undertaken in recent years.

< **Figure 24**>

A wide variety of nickel complexes containing N^N^N ligands based on a 2-arylimino-pyridine linked at the 6-position by benzimidazolyl or benzoxazolyl unit have been reported and assessed as pre-catalysts in oligo-/polymerization (**46**, Fig. 24) [92, 112-115]. On addition of Et_2AlCl, all examples of **46** exhibited good catalytic activities up to 10^6 g mol^{-1}(Ni) h^{-1} for ethylene oligomerization. More specifically, N-methylated **46** (Z = N-Me) showed better catalytic activities (up to 5.87×10^5 g mol^{-1}(Ni) h^{-1} atm^{-1}) [92] than their N-propylated **46** (Z = N-*i*Pr) [112]. When benzimidazole is replaced by benzoxazole, **46** (Z = O) [113] showed improved activities in comparison to the pre-catalysts containing a N-methyl or N-isopropyl-substituent on the benzimidazole ring [92,112,113]. Complexes **46**, containing N–H on the benzimidazole ring [114,115], displayed a higher activity (10^6 g mol^{-1}(Ni) h^{-1}) than the N-alkylated **46** [110,111]. In addition, complexes containing electron withdrawing substituents at the N-aryl group showed lower activity than that with alkyl substituents [92,112-115]. As has been observed elsewhere the addition of PPh_3 resulted in better catalytic activities toward ethylene oligomerization; a plausible role of the PPh_3 is to stabilize the catalytically active species while being labile enough to provide a site for ethylene coordination [92, 112-113].

< **Figure 25**>

Bis(imino)pyridine-nickel complexes, **47**, have also been the subject of investigations directed towards probing catalytic performance in ethylene oligomerization. In particular, unsymmetrical examples of **47**, in which one N-aryl group is substituted at its 2,6-position by benzhydryl groups have been explored (Fig. 25) [116]. When activated with EASC, **47** could be easily activated and showed high activities up to 2.5×10^6 g

mol^{-1}(Ni) h^{-1} for ethylene oligomerization with moderate to good selectivities for 1-butene (54.2-99.1%) at 10 atmospheres of ethylene pressure [116].

< **Figure 26**>

The Casagrande Jr. group studied the ethylene oligomerization properties of two examples of nickel-containing **48** bearing an N^N^N-ligand based on a monoanionic pyrrolide-imine-amine (Fig. 26) [117]. When activated with 250 equivalents of MAO, **48a** showed moderate activity [TOF = 1.16×10^4 mol (C_2H_4) mol^{-1}(Ni) h^{-1}] along with good selectivity towards 1-butene (89 wt%). Increasing the steric hindrance on the pyrrolide unit, as in **48b**, caused an increase in the activity by a factor of 2.50, suggesting that the tert-butyl substituent acts as a protecting group for the active species, thereby increasing the catalytic productivity [29,117]. The use of EASC instead of MAO afforded a highly active species, however the 1-butene selectivity was drastically reduced.

Ojwach and co-workers have explored the use of cationic **49**, chelated by two pyridinylaminoamine ligands, as an oligomerization pre-catalyst (Fig. 27) [118]. Upon activation with either $EtAlCl_2$ or MAO, **49** exhibited a high catalytic activity of 2.74×10^6 g oligomer mol^{-1} (Ni) h^{-1} and produced mostly ethylene dimers (C_4), in addition to some trimers (C_6) and tetramers (C_8) [118].

< **Figure 27**>

4. Dinuclear nickel pre-catalysts

In addition to the mononuclear nickel pre-catalysts described above, the potential for synergic effects promoted by the presence of two catalytic active species held in close proximity has continued to attract attention [26].

< **Figure 28**>

The methylene-bridged bimetallic α-diimine nickel(II) complexes, **50a-f**, prepared in our laboratory, were studied as pre-catalysts for the polymerization of ethylene (Fig. 28) [71]. On activation with either Et_2AlCl or MAO, **50a-f** exhibited high activities (up to

7.86 × 10^6 g (PE) mol^{-1}(Ni) h^{-1}) over the temperature range, ambient to 50 °C. The substitution pattern present on the terminal N-aryl groups of the compartmental ligand significantly affected the catalytic activities and were found to vary in the order: **50d** (2,4,6-tri(Me)) > **50a** (2,6-di(Me)) > **50e** (2,6-di(Et)-4-Me) > **50b** (2,6-di(Et)) > **50c** (2,6-(i-Pr)). The chloride complex **50f** exhibited a slightly lower activity than its bromide analogue **50d**. Most notably, the binuclear complexes **50a-f** showed a positive synergic effect by displaying higher activity than the mononuclear analogue **17a** (Fig. 7) [71].

< **Figure 29**>

Chen and Fu *et al.* have investigated the catalytic performance of the binuclear nickel complexes, **51a** and **51b**, supported by the conjugated bis(α-diimine) ligands (Fig. 29) [119]. Both complexes, when activated by MMAO, generate highly active ethylene polymerization catalysts with activities up to 1.05 × 10^6 g(PE) mol^{-1} (Ni) h^{-1} [119].

< **Figure 30**>

Our group has also explored the capacity of the binuclear nickel complexes **52a** and **52b**, supported by the 4,5,9,10-tetra(arylimino)pyrenylidenes, to mediate ethylene polymerization (Fig. 30) [120]. Both **52a** and **52b** exhibited high activities towards ethylene polymerization in the presence of either MAO or Me_2AlCl, maintaining this good performance over a prolonged period (notably longer than previously reported for di-nickel pre-catalysts) [120]. When in the presence of MAO, **52a** showed the highest activity up to 1.5 × 10^6 g(PE) mol^{-1} (Ni) h^{-1} and required less co-catalyst than observed for the mononuclear catalyst **6** (Fig. 3) [54]. In general, the polyethylenes obtained revealed less branches than observed for the mononuclear analogues **6** (Scheme 3) [54] and other related dinickel complexes **51** (Fig. 29) [120].

Zohuri *et al.* have studied the performance of the aryl-linked bis(α-diimine)-dinickel complexes, **53a-d**, as pre-catalysts in ethylene polymerization (Fig. 31) [121]. Upon activation with MAO, **53a-d** were all active and **53d** showed the highest activity (up to 1.07 × 10^6 g(PE) mol^{-1}(Ni) h^{-1}) of the four systems screened [121].

< **Figure 31**>

Solan and co-workers have reported the dinickel salts **54** (X = Cl, Br), supported by the bis(iminopyridyl)phthalazine compartmental ligand, as modestly active pre-catalysts in ethylene oligomerization (Fig. 32) [122]. Both complexes, on activation by MAO, formed low molecular weight waxes with methyl-branched products predominating.

< **Figure 32**>

The heteronuclear Ni-Co complexes, **55a-e**, supported by the 2-methyl-2,4-bis(6-aryliminopyridin-2-yl)-1H-1,5-benzodiazepine compartmental ligand, have been reported by our group (Fig. 33) [123]. In the presence of MMAO, these mixed-metal complexes showed good activities towards ethylene oligomerization. Unfortunately, they all showed less activity than their mononuclear cobalt analogues [123]. Of the five Ni-Co complexes screened, **55d**, displayed the highest activity which has been attributed to the cumulative effects of electronic and steric properties of the ligand. Interestingly, the oligomeric materials obtained followed a Poisson distribution; notably formed without the presence of $ZnEt_2$.

< **Figure 33**>

Methylene-bridged bis(pyridinyliminenickel) complexes have also shown some potential as pre-catalysts in polymerization applications (Fig. 34) [124]. For example **56a-h**, on activation with MAO, display high catalytic activities 10^6 g(PE) mol^{-1}(Ni) h^{-1}. However, these type of catalyst show poor selectivity by affording both polyethylenes and oligomers. It is likely that activation with the co-catalyst generates multiple nickel active sites that can promote the formation of products with different molecular weights.

< **Figure 34**>

5. Conclusions and outlook

The discovery of α-diimine-nickel(II) catalysts by Brookhart and co-workers more than two decades ago has proved to be a milestone in the evolution of late transition

metal catalysts for the polymerization of ethylene. Recent progress highlighted in this work has shown that this relatively mature field still has plenty of opportunities for new and exciting technological advances to be made using nickel-based homogeneous catalysis. Though skillful and imaginative ligand design, catalysts have been developed that can now exhibit excellent thermal stability at industrially relevant operating temperatures generating high molecular weight polymers through to well-defined carbon content α-olefins. What is more, these catalysts can be tuned (*via* ligand variation and operating conditions, *e.g.*, temperature) to afford linear through to highly branched polyethylenes with narrow polydispersities. While the original ideas of steric and electronic control on catalyst performance through N-aryl and ligand backbone variation are still highly relevant, new concepts such as ring strain have emerged that have opened the door to new exceptionally active and well-behaved catalysts delivering polyethylenes of industrial importance. Notably, the formation of hyperbranched polethylenes displaying properties characteristic of thermoplastic elastomers (TPEs) show great promise for these materials to be employed as alternatives to elastomeric ethylene copolymers.

Acknowledgements

This work is supported by the National Natural Science Foundation of China (21374123, 21476060, and U1362204). G.A.S. thanks the Chinese Academy of Sciences for a Visiting Scientist Fellowship.

GLOSSARY

BAF^-	Tetrakis[3,5-bis(trifluoromethyl)phenyl]borate
EASC ($Et_3Al_2Cl_3$)	Ethyl aluminum sesquichloride
Et_2AlCl (DEAC)	Diethylaluminum chloride
Et_3Al	Triethylaluminum

HDPE	High-density polyethylene
LLDPE	Linear low-density polyethylene
MA	Methyl acrylate
MAO	Methylaluminoxane
MMA	Methyl methacrylate
MMAO	Modified methylaluminoxane
M_n	Number-average molecular weight
M_w	Weight-average molecular weight
MWD	Molecular weight distribution
PDI	Polydispersity index
PE	Polyethylene
PNB	Polynorbornene
PMMA	Polymethyl methacrylate
T_m	Melting temperature
TOF	Turnover frequency
TPE	Thermoplastic elastomer

References

[1] J. Skupinska, Chem. Rev. 91 (1991) 613-648.

[2] L. K. Johnson, C. M. Killian, M. Brookhart, J. Am. Chem. Soc. 117 (1995) 6414-6415.

[3] S. D. Ittel, L. K. Johnson, M. Brookhart, Chem. Rev. 100 (2000) 1169-1203.

[4] A. Nakamura, S. Ito, K. Nozaki, Chem. Rev. 109 (2009) 5215-5244.

[5] E. Y. X. Chen, Chem. Rev. 109 (2009) 5157-5214.

[6] W. Li, X. Zhang, A. Meetsma, B. Hessen, J. Am. Chem. Soc. 126 (2004) 12246-12247.

[7] C. L. Chen, S. J. Luo, R. F. Jordan, J. Am. Chem. Soc. 130 (2008) 12892-12893.

[8] C. L. Chen, R. F. Jordan, J. Am. Chem. Soc. 132 (2010) 10254-10255.

[9] C. L. Chen, S. J. Luo, R. F. Jordan, J. Am. Chem. Soc. 132 (2010) 5273-5284.

[10] W. C. A., Jr., J. L. Rhinehart, A. G. Tennyson, B. K. Long, J. Am. Chem. Soc. 138 (2016) 774-777.

[11] W. C.A. Jr., B. K. Long, ACS Macro Lett. 5 (2016) 1029-1033.

[12] Z. Chen, K. E. Allen, P. S. White, O. Daugulis, M. Brookhart, Organometallics 35 (2016) 1756-1760.

[13] B. L. Small, M. Brookhart, A.M. A. Bennet, J. Am. Chem. Soc. 120 (1998) 4049-4050.

[14] G. J. P. Britovsek, V. C. Gibson, B. S. Kimberley, P. J. Maddox, S. J. McTavish, G. A. Solan, A. J. P.

Whitea, D. J. Williams, Chem. Commun. 7 (1998) 849-850.
[15] G. J. P. Britovsek, V. C. Gibson and D. F. Wass, Angew. Chem., Int. Ed. 38 (1999) 428-447.
[16] V. C. Gibson, C. Redshaw, G. A. Solan, Chem. Rev. 107 (2007) 1745-1776.
[17] C. Bianchini, G. Giambastiani,I. G. Rios, G. Mantovani, A. Meli, A. M. Segarra, Coord. Chem. Rev. 250 (2006) 1391-1418.
[18] Z. Flisak, W.-H. Sun. ACS Catal. 5(2015) 4713-4724.
[19] S. Jie, W.-H. Sun, T. Xiao, Chin. J. Polym. Sci. 28 (2010) 299-304.
[20] T. Xiao, W. Zhang, J. Lai, W.-H. Sun, C. R. Chim. 14 (2011) 851-855.
[21] W. Zhang, W.-H. Sun, C. Redshaw, Dalton Trans. 42 (2013) 8988-8997.
[22] V. C. Gibson, G. A. Solan, in Catalysis without Precious Metals (Ed. M. Bullock), Wiley-VCH, Weinheim, 2010, 111-141.
[23] V. C. Gibson, G. A. Solan, Top. Organomet. Chem. 26 (2009) 107-158.
[24] S. Wang, W.-H. Sun, C. Redshaw, J. Organomet. Chem. 751 (2014) 717-741.
[25] S. Budagumpi, K.-H. Kim, I. Kim, Coord. Chem. Rev. 255 (2011) 2785-2809.
[26] R. Gao, W.-H. Sun, C. Redshaw, Catal. Sci. Technol. 3 (2013) 1172-1179.
[27] C.M. Killian, L.K. Johnson, M. Brookhart, Organometallics 16 (1997) 2005-2007.
[28] S.A. Svefda, M. Brookhart, Organometallics 18 (1999) 65-74.
[29] L. P. Moeti, J. Darkwa, S. Afr. J. Chem. 69 (2016) 236-243.
[30] F. Speiser, P. Braunstein, L. Saussine, Acc Chem Res, 38 (2005), 784-793.
[31] F. Speiser, P. Braunstein, L. Saussine, R. Welter, Inorg Chem. 43 (2004), 1649-1658.
[32] F. Speiser, P. Braunstein, L. Saussine, R. Welter, Organometallics 23 (2004), 2613-2624.
[33] F. Speiser, P. Braunstein, Organometallics 2004, 23, 2633-2640.
[34] S. Zhang, R. Pattacini, S. Jie, P. Braunstein, Dalton Trans. 41 (2012) 379-386.
[35] A. Kermagoret, P. Braunstein, Dalton Trans. (2008) 822-831.
[36] A. Kermagoret, F. Tomicki, P. Braunstein, Dalton Trans. (2008) 2945-2955.
[37] P. Chavez, I. G. Rios, A. Kermagoret, R. Pattacini, A. Meli, C. Bianchini, G. Giambastiani, P. Braunstein, Organometallics 28 (2009) 1776-1784.
[38] A. Hamada, P. Braunstein, Inorg. Chem. 48 (2009) 1624-1637.
[39] A. Boudier, P.-A.R. Breuil, L. Magna, H. Olivier-Bourbigou, P. Braunstein, J. Organomet. Chem. 718 (2012) 31-37.
[40] A. Ghisolfi, C. Fliedel, V. Rosa, K.Y. Monakhov, P. Braunstein, Organometallics 33 (2014) 2523-2534.
[41] J. P. Taquet, O. Siri, P. Braunstein, R. Welter, Inorg Chem. 45 (2006), 4668-4676.
[42] D. Schweinfurth, C. Y. Su, S. C. Wei, P. Braunstein, B. Sarkar, Dalton Trans. 41 (2012) 12984-12990.
[43] S. Hameury, P. de Frémont, P.-A.R. Breuil, H. Olivier-Bourbigou, P. Braunstein, Organometallics 34 (2015) 2183-2201.
[44] A. Boudier, P.-A. R. Breuil, L. Magna, H. Olivier-Bourbigou, P. Braunstein, Chem. Commun. 50 (2014) 1398-1407.
[45] A. Boudier, P.-A. R. Breuil, L. Magna, H. Olivier-Bourbigou, P. Braunstein, Dalton Trans. 44 (2015) 12995-12998.
[46] D. P. Gates, S. A. Svejda, E. Oñate, C. M. Killian, L. K. Johnson, P. S. White, M. Brookhart,

Macromolecules 33 (2000) 2320-2334.
[47] S. A. Svejda, L. K. Johnson, M. Brookhart, J. Am. Chem. Soc. 121 (1999) 10634-10635.
[48] M. D. Leatherman, S. A. Svejda, L. K. Johnson, M. Brookhart, J. Am. Chem. Soc. 125 (2003) 3068.
[49] A. Michalak, T. Ziegler, Organometallics 22 (2003) 2069-2079.
[50] F.-S. Liu, H.-B. Hu, Y. Xu, L.-H. Guo, S.-B. Zai, K.-M. Song, H.-Y. Gao, L. Zhang, F. M. Zhu, Q. Wu, Macromolecules 42 (2009) 7789-7796.
[51] H. Gao, H. Hu, F. Zhua, Q. Wu, Chem. Commun. 48 (2012) 3312-3314.
[52] M. M. Wegner, A. K. Ott, B. Rieger, Macromolecules, 43 (2010) 3624-3633.
[53] L. Li, M. Jeon, S. Y. Kim, J. Mol. Catal. A: Chem. 303 (2009) 110-116.
[54] K. Song, W. Yang, B. Li, Q. Liu, C. Redshaw, Y. Li, W.-H. Sun, Dalton Trans. 42 (2013) 9166-9175.
[55] D. J. Tempel, L. K. Johnson, R. L. Huff, P. S. White, M. Brookhart, J. Am. Chem. Soc. 122 (2000) 6686-6700.
[56] D. H. Camacho, E. V. Salo, J. W. Ziller, Z. Guan, Angew. Chem. Int. Ed. 43 (2004) 1821-1825.
[57] C. S. Popeney, A. L. Rheingold, Z. Guan, Organometallics 28 (2009) 4452-4463.
[58] D. H. Camacho, E. V. Salo, Z. Guan, J. W. Ziller, Organometallics 24 (2005) 4933-4939.
[59] D. H. Leung, J. W. Ziller, Z. Guan, J. Am. Chem. Soc. 130 (2008) 7538-7539.
[60] D. Jia, W. Zhang, W. Liu, L. Wang, C. Redshaw, W. -H. Sun,. Catal. Sci. Technol. 3 (2013) 2737-2745.
[61] Q. Liu, W. Zhang, D. Jia, X. Hao, C. Redshaw, W. -H. Sun, Appl. Catal. A: Gen. 475 (2014) 195-202.
[62] M. Gao, S. Du, Q. Ban, Q. Xing, W. -H. Sun, J. Organomet. Chem. 798 (2015) 401-407.
[63] H. Liu, W. Zhao, X. Hao, C. Redshaw, W. Huang, W.-H. Sun,. Organometallics 30 (2011) 2418-2424.
[64] S. Kong, C.-Y. Guo, W. Yang, L. Wang, W.-H. Sun, R. Glaser,. J. Organomet. Chem. 725 (2013) 37-45.
[65] L. Fan, S. Du, C.-Y. Guo, X. Hao, W.-H. Sun, J. Polym. Sci. Part A: Polym. Chem. 53 (2015) 1369-1378.
[66] Q. Mahmood, Y. Zeng, X. Wang, Y. Sun, W.-H. Sun, Dalton Trans. 46 (2017) DOI: 10.1039/c7dt01295k.
[67] H. Liu, W. Zhao, J. Yu, W. Yang, X. Hao, C. Redshaw, L. Chen, W.-H. Sun, Catal. Sci. Technol. 2 (2012) 415-422.
[68] L. Fan, E. Yue, S. Du, C.-Y. Guo, X. Hao, W.-H. Sun, RSC Adv. 5 (2015) 93274-93282.
[69] X. Wang, L. Fan, Y. Ma, C.-Y. Guo, G. A. Solan, Y. Sun, W.-H. Sun, Polym. Chem. 8 (2017), DOI: 10.1039/C7PY00434.
[70] C. Wen, S. Yuan, Q. Shi, E. Yue, D. Liu, W.-H. Sun, Organometallics 33 (2014) 7223-7231.
[71] S. Kong, K. Song, T. Liang, C-Y. Guo, W.-H. Sun, C. Redshaw, Dalton Trans. 42 (2013) 9176-9187.
[72] S. Du, S. Kong, Q. Shi, J. Mao, C. Guo, J. Yi, T. Liang, W.-H. Sun, Organometallics 34 (2015) 582-590.
[73] Z. Guan, P. M. Cotts, E. F. McCord, S. J. McLain, Science, 283 (1999) 2059-2062.
[74] S. Du, Q. Xing, Z. Flisak, E. Yue, Y. Sun, W.-H. Sun, Dalton Trans. 44 (2015) 12282-12291.
[75] X. Wang, L. Fan, Y. Yuan, S. Du, Y. Sun, G. A. Solan, C.-Y. Gao, W.-H. Sun, Dalton Trans. 45 (2016) 18313-18323.
[76] S. Yuan, E. Yue, C. Wen, W.-H. Sun, RSC Adv. 6 (2016) 7431-7438.
[77] Y. Chen, S. Du, C. Huang, G. A. Solan, X. Hao,W.-H. Sun, J. Polym. Sci. Part A: Polym. Chem.

55(2017) 1971–1983.
[78] J. L. Rhinehart, L. A. Brown, B. K. Long, J. Am. Chem. Soc. 135 (2013) 16316-16319.
[79] J. L. Rhinehart, N. E. Mitchell, B. K. Long, ACS Catal. 4 (2014) 2501-2504.
[80] L. A. Rishina, Y. V. Kissin, S. S. Lalayan, S. C. Gagieva, D. A. Kurmaev, V. A. Tuskaev, B. M. Bulychev, J. Mol. Cat. A: Chem.423 (2016) 495-502.
[81] W.-H. Sun, S. Song, B. Li, C. Redshaw, X. Hao, Y-S. Li, F. Wanga, Dalton Trans. 41 (2012) 119909-12312.
[82] H. Suo, T. Zhao, Y. Wang, Q. Ban, W.-H. Sun, Molecules, 22 (2017) 630.
[83] S. Zai, F. Liu, H. Gao, C. Li, G. Zhou, S. Cheng, L. Guo, L. Zhang, F. Zhu, Q. Wu, Chem. Commun. 46 (2010) 4321-4323.
[84] S. Zai, H. Gao, Z. Huang, H. Hu, H. Wu, Q. Wu, ACS Catal. 2 (2012) 433-440.
[85] E. Yue, L. Zhang, Q. Xing, X. Cao, X. Hao, C. Redshaw, W.-H. Sun, Dalton Trans. 43 (2014) 423-431.
[86] E. Yue, Q. Xing, L. Zhang, Q. Shi, X. Cao, L. Wang, C. Redshaw, W.-H. Sun, Dalton Trans. 43 (2014) 3339-3346.
[87] A. A. Antonov, N. V. Semikolenova, E. P. Talsi, M. A. Matsko, V. A. Zakharov, K. P. Bryliakov J. Organomet. Chem. 822 (2016) 241-249.
[88] K. Kumar, T.e Godeto, J. Darkwa, J. Organomet. Chem. 818 (2016) 137-144.
[89] C. Obuah, J. H. L. Jordaan, J. Darkwa, Catal. Sci. Technol. 6 (2016) 4814-4823.
[90] S. Song, T. Xiao, T. Liang, F. Wang, C. Redshaw, W.-H. Sun, Catal. Sci. Technol. 1 (2011) 69-75.
[91] S. Song, Y. Li, C. Redshaw, F. Wang, W.-H. Sun, J. Organomet. Chem. 696 (2011) 3772-3778.
[92] P. Hao, S. Zhang, W.-H. Sun, Q. Shi, S. Adewuyi, X. Lu, P. Li, Organometallics 26 (2007) 2439-2446.
[93] R. Gao, L. Xiao, X. Hao, W.-H. Sun, F. Wang, Dalton Trans. (2008) 5645-5651.
[94] J. Yu, X. Hu, Y. Zeng, L. Zhang, C. Ni, X. Hao, W.-H. Sun, New J. Chem. 35 (2011) 178-183.
[95] X. Hou, T. Liang, W.-H. Sun, C. Redshaw, X. Chen, J. Organomet. Chem. 708-709 (2012) 98-105.
[96] W. Chai, J. Yu, L. Wang, X. Hu, C. Redshaw, W.-H. Sun, Inorg. Chim. Acta. 385 (2012) 21-26.
[97] L. Zhang, E. Castillejos, P. Serp, W.-H. Sun, J. Durand, Catal. Today 235 (2014) 33-40.
[98] Z. Sun, E. Yue, M. Qu, I. V. Oleynik, I. I. Oleynik, K. Li, T. Liang, W. Zhang, W.-H. Sun, Inorg. Chem. Front. 2 (2015) 223-227.
[99] J. Yu, Y. Zeng, W. Huang, X. Hao, W.-H. Sun, Dalton Trans. 40 (2011) 8436-8443.
[100] X. Hou, Z. Cai, X. Chen, L. Wang, C. Redshaw, W.-H. Sun, Dalton Trans. 41 (2012) 1617-1623.
[101] L. Zhang, X. Hao, W.-H. Sun, C. Redshaw, ACS Catal. 1 (2011) 1213-1220.
[102] I. E. Soshnikov, N. V. Semikolenova, K. P. Bryliakov, V.A. Zakharov, W.-H. Sun, E. P. Talsi, Organometallics 34 (2015) 3222-3227.
[103] E. Yue, Y. Zeng, W. Zhang, F. Huang, X.-P. Cao, T. Liang, W.-H. Sun, Inorg. Chim. Acta 442 (2016) 178-186.
[104] Y. Zeng, Q. Mahmood, X. Hao, W.-H. Sun, J. Polym. Sci. Part A: Polym. Chem. 55 (2017) 1910-1919.
[105] S. Wang, S. Du, W. Zhang, S. Asuha, W-H. Sun, Chem. Open 4 (2015) 328-334.
[106] S. Wang, W. Zhang, S. Du, S. Asuha, Z. Flisak, W-H. Sun, J. Organomet. Chem. 798 (2015) 408-413.
[107] F. Huang, Z. Sun, S. Du, E. Yue, J. Ba, X. Hu, T. Liang, G. B. Galland, W.-H. Sun, Dalton Trans. 44

(2015) 14281-14292.
[108] Z. Sun, F. Huang, M. Qu, E. Yue, I. V. Oleynik, I. I. Oleynik, Y. Zeng, T. Liang, K. Li, W. Zhang, W.-H. Sun, RSC Adv. 5 (2015) 77913-77921.
[109] C. Huang, Y. Zhang, T. Liang, Z. Zhao, X. Hu, W.-H. Sun, New J. Chem. 40 (2016) 9329-9336.
[110] C. Huang, Y. Zeng, Z. Flisak, Z. Zhao, T. Liang, W.-H. Sun, J. Polym. Sci. Part A: Polym. Chem. 55 (2017) 2071–2083.
[111] Y. Zhang, C. Huang, X. Wang, Q. Mahmood, X. Hao, X. Hu, C.-Y. Guo, G. A. Solan, W.-H. Sun, Polym. Chem. 8 (2017) 995-1005.
[112] Y. Chen, P. Hao, W. Zuo, K. Gao, W.-H. Sun, J. Organomet. Chem. 693 (2008) 1829-1840.
[113] R. G, M. Zhang, T. Liang, F. Wang, W.-H. Sun, Organometallics 27 (2008) 5641-5648.
[114] L. Xiao, M. Zhang, R. Gao, X. Cao, W.-H. Sun, Aust. J. Chem. 63 (2010) 109-115.
[115] X. Chen, L. Zhang, J. Yu, X. Hao, H. Liu, W.-H. Sun, Inorg. Chim. Acta 370 (2011) 156-163.
[116] J. Lai, X. Hou, Y. Liu, C. Redshaw, W.-H. Sun, J. Organomet. Chem. 702 (2012) 52-58.
[117] A. C. Pinheiro, A. H. Virgili, T. Roisnel, E. Kirillov, J.-F. Carpentier, O. L. Casagrande Jr., RSC Adv. 5 (2015) 91524-91531.
[118] G. S. Nyamato, S. O. Ojwach, M. P. Akerman, Dalton Trans. 45 (2016) 3407-3416.
[119] L. Zhu, Z. Fu, H. Pan, W. Feng, C. Chen, Z.-Q. Fan, Dalton Trans. 43 (2014) 2900-2906.
[120] Q. Xing, K. Song, T. Liang, Q. Liu, W.-H. Sun, C. Redshaw, Dalton Trans. 43 (2014) 7830-7837.
[121] M. Khoshsefat, G. H. Zohuri, N. Ramezanian, S. Ahmadjo, M. Haghpanah, J. Polym. Sci., Part A: Polym. Chem. 54 (2016) 3000-3011.
[122] N. Savjani, K. Singh, G. A. Solan, Inorg. Chim. Acta 436 (2015) 184-194.
[123] S. Zhang, Q. Xing, W.-H. Sun, RSC Adv. 6 (2016) 72170-72176.
[124] S. Jie, D. Zhang, T. Zhang, W.-H. Sun, J. Chen, Q. Ren, D. Liu, G. Zheng, W. Chen, J. Organomet. Chem. 690 (2005) 1739-1749.

Captions for Schemes, Tables and Figures

Scheme 1. Proposed intermediate formed in the activation of the 8-mesitylimino-5,6,7-tetrahydroquinoline-nickel pre-catalyst, **37e**, with $AlEt_2Cl$ [102]

Scheme 2. Imine–enamine tautomerization on aniline condensation [109]

Table 1 Variation in polyethylene properties as a function of the pre-catalyst structure and temperature; MAO activation[a]

Table 2 Variation in polyethylene properties as a function of the pre-catalyst structure and temperature; Et_2AlCl activation[a]

Fig. 1. Brookhart's original α-diimine-nickel catalysts, **1a-e** [2, 46]

Fig. 2. Skeletal modifications in α-diimine-nickel pre-catalysts, **2a-c** [48-49]

Fig. 3. N-aryl and backbone variations in α-diimine-nickel pre-catalysts, **3-6** [52-54]

Fig. 4. Macrocyclic α-diimine-nickel pre-catalysts, **7-10** [56-59]

Fig. 5. Benzhydryl-containing unsymmetrical and symmetrical α-diimine-nickel pre-catalysts, **11-13** [60-62]

Fig. 6. Benzhydryl-containing unsymmetrical diiminoacenaphthene-nickel pre-catalysts, **14** and **15** [63-69]

Fig. 7. Diiminoacenaphthene-type α-diimine pre-catalysts, **16-18** [70-74]

Fig. 8. Difluorobenzhydryl-substituted diiminoacenaphthene-nickel pre-catalysts, **19-22** [75-77]

Fig. 9. 2,6-Dibenzhydryl-substituted α-diimine-nickel pre-catalysts, **23** and **24** [78,79]

Fig. 10. Fluoro- and trifluoromethyl-substituted α-diimine-nickel pre-catalysts, **25** [80]

Fig. 11. Pyridinyl-imine and -amine pre-catalysts, **26** and **27** [81-84]

Fig. 12. Sterically bulky N-naphthyl-containing pyridinylimine-nickel pre-catalysts, **28** [85-86]

Fig. 13. CF_3- and F-substituted pyridinylimine-nickel pre-catalysts, **29** and **30** [87]

Fig. 14. Alkoxysilyl-containing pyridinylimine-nickel pre-catalysts, **31** and **32** [88]

Fig. 15. Pridinylpyrazolyl- and pyridinyltriazole-nickel pre-catalysts, **33** [89] and **34** [42]

Fig. 16. Quinolinylimine pre-catalysts, **35** [90-91]

Fig. 17. Pyridinylbenzimidazole- and pyridinylbenzoxazole-nickel pre-catalysts, **36** [92-93]

Fig. 18. 8-Arylimino-5,6,7-tetrahydroquinoline-nickel pre-catalysts, **37** and **38** [94-101]

Fig. 19. Benzhydryl-substituted 8-naphthylimino-5,6,7-tetrahydroquinoline pre-catalyst, **39** [103]

Fig. 20. Fluorenyl-substituted 8-arylimino-5,6,7-tetrahydroquinoline pre-catalysts, **40** [104]

Fig. 21. 4-Arylimino-1,2,3-trihydroacridyl-nickel pre-catalysts, **41** [105,106]

Fig. 22. Iminocyclohepta- and iminocyclohexa-pyridine-nickel pre-catalysts, **42**, **43a** and **43b** [107-110]

Fig. 23. Imino-cyclopenta[b]pyridine-nickel pre-catalysts, **44** and **45** [111]

Fig. 24. 2-Imino-6-benzimidazolyl/benzoxazolyl-pyridine-nickel pre-catalysts, **46** [92,112-115]

Fig. 25. Unsymmetrical bis(imino)pyridine-nickel pre-catalysts, **47** [116]

Fig. 26. Pyrrolide-imine-amine-nickel pre-catalysts, **48** [117]

Fig. 27. Cationic pyridinylaminoamine-nickel pre-catalyst, **49** [118]

Fig. 28. Methylene-bridged dinickel bis(α-diimine) pre-catalysts, **50a-f** [71]

Fig. 29. Bis(α-diimine) dinuclear nickel pre-catalysts, **51a** and **51b** [119]

Fig. 30. Pyrenylidene-bridged bis(α-diimine)-dinickel pre-catalysts, **52a** and **52b** [120]

Fig. 31. Aryl-linked bis(α-diimine)-dinickel pre-catalysts, **53a-d** [121]

Fig. 32. Bis(iminopyridyl)phthalazine-dinickel pre-catalysts, **54** [122]

Fig. 33. Heteronuclear Ni-Co pre-catalysts, **55a-e** [123]

Fig. 34. Methylene-bridged bis(pyridinyliminonickel) pre-catalysts, **56a-h** [124]

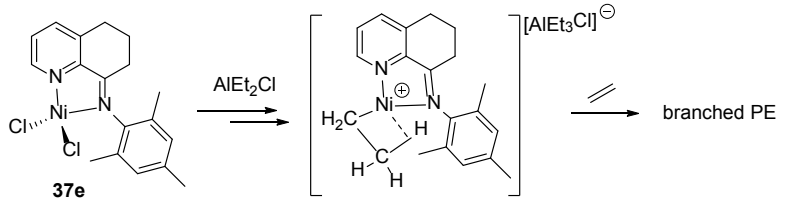

Scheme 1. Proposed intermediate formed in the activation of the 8-mesitylimino-5,6,7-tetrahydroquinoline-nickel pre-catalyst, **37e**, with $AlEt_2Cl$ [102]

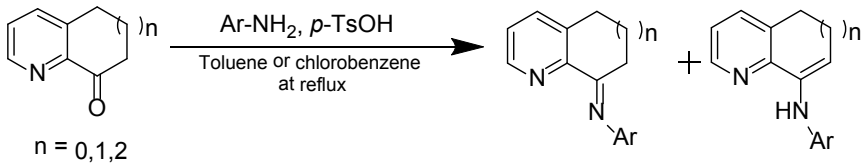

Scheme 2. Imine–enamine tautomerization on aniline condensation [109]

Table 1 Variation in polyethylene properties as a function of the pre-catalyst structure and temperature; MAO activation[a]

Pre-catalyst	Temp /°C	M_w[b]	M_w/M_n[b]	Branching content[c]	T_m /°C[d]	ref.
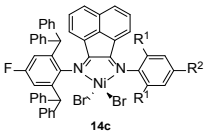 14c	30	7.69	2.20	132	52.7	65
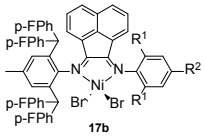 17b	30	4.33	1.80	113	55.3	72
	50	2.88	2.36	140	45.4	
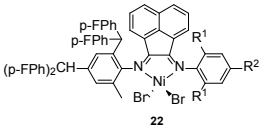 22	30	2.24	3.17	44	99.5	77
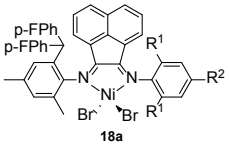 18a	30	2.60	2.70	27	111.8	74
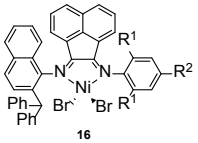 16	30	3.51	2.70	17	124.3	70
	60	2.81	2.00	42	102.4	

[a] Ethylene pressure 10 atm., toluene as solvent and MAO as activator. [b] Determined by GPC, M_w : 10^5 g mol^{-1}. [c] Determined by ^{13}C NMR spectroscopy and is the number of branches per 1000 carbons or estimated by FT-IR spectroscopy. [d] Determined by DSC.

Table 2 Variation in polyethylene properties as a function of the pre-catalyst structure and temperature; Et_2AlCl activation[a]

Pre-catalyst	Temp /°C	M_w[b]	M_w/M_n[b]	Branching content[c]	T_m/°C[d]	ref.
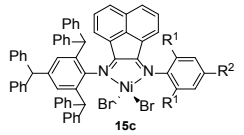 15c	30	5.83	2.80	135	60.8	69
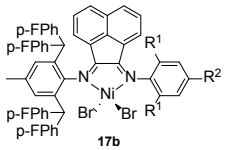 17b	30	3.66	2.70	95	51.4	72
	50	3.28	2.25	150	43.5	
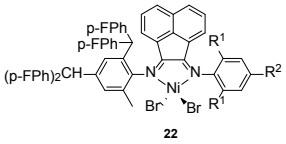 22	30	2.99	3.14	38	100.4	77
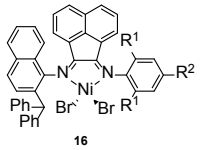 16	30	3.34	2.70	24	131.0	70

[a] Ethylene pressure 10 atm., toluene as solvent and Et_2AlCl as activator. [b] Determined by GPC, M_w : 10^5g mol^{-1}. [c] Determined by ^{13}C NMR spectroscopy and is the number of branches per 1000 carbons or estimated by FT-IR spectroscopya. [d] Determined by DSC.

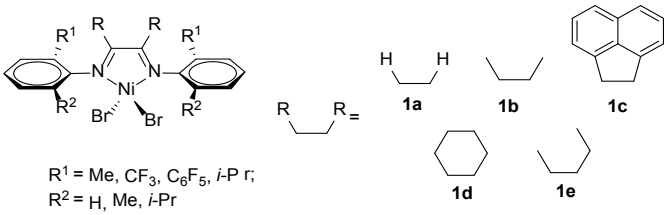

Fig. 1. Brookhart's original α-diimine-nickel catalysts, **1a-e** [2, 46]

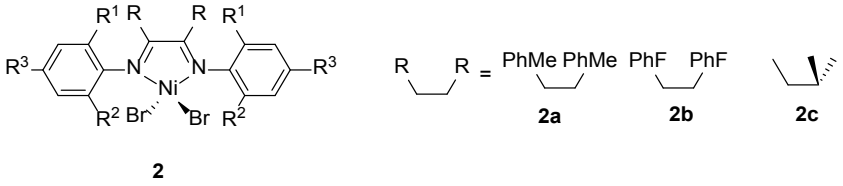

Fig. 2. Skeletal modifications in α-diimine-nickel pre-catalysts, **2a-c** [48-49]

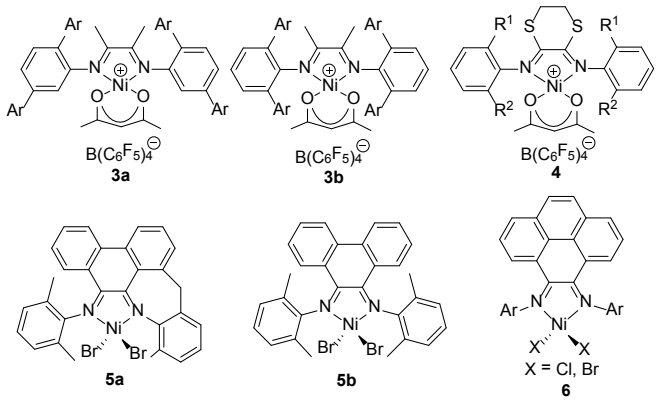

Fig. 3. N-aryl and backbone variations in α-diimine-nickel pre-catalysts, **3-6** [52-54]

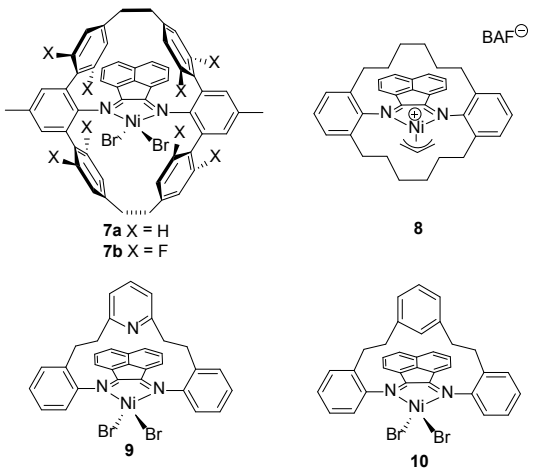

Fig. 4. Macrocyclic α-diimine-nickel pre-catalysts, **7**-**10** [56-59]

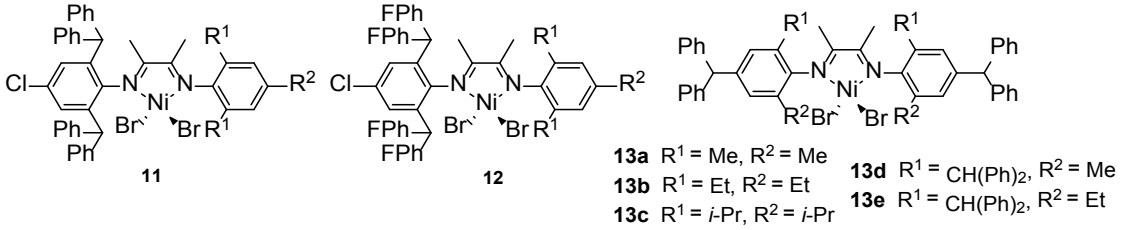

Fig. 5. Benzhydryl-containing unsymmetrical and symmetrical α-diimine-nickel pre-catalysts, **11**-**13** [60-62]

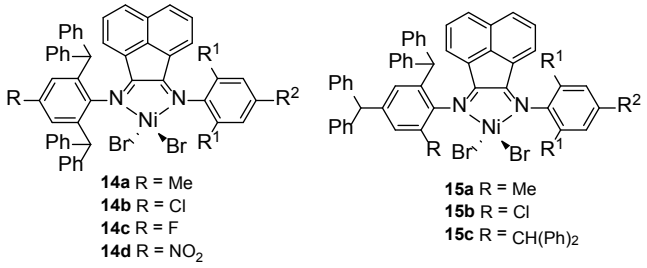

Fig. 6. Benzhydryl-containing unsymmetrical diiminoacenaphthene-nickel pre-catalysts, **14** and **15** [63-69]

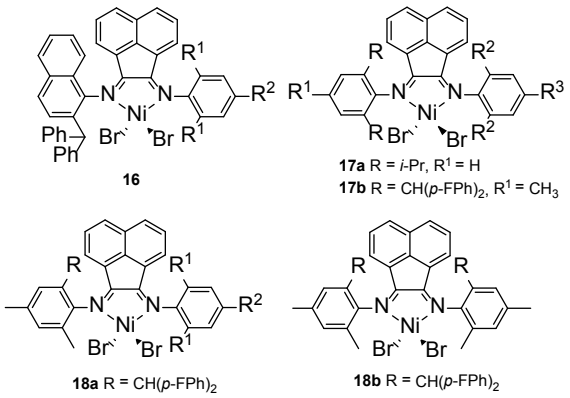

Fig. 7. Diiminoacenaphthene-type α-diimine pre-catalysts, **16-18** [70-74]

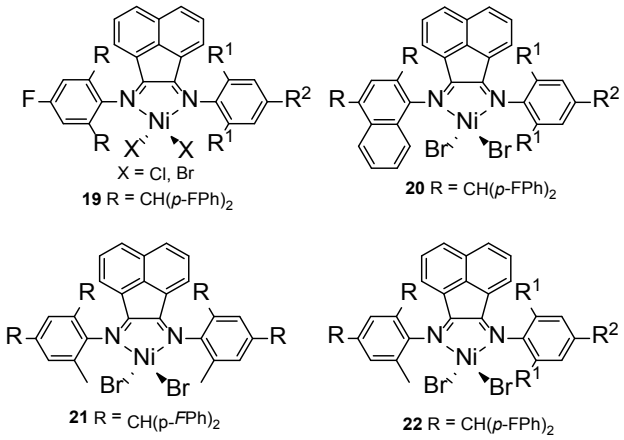

Fig. 8. Difluorobenzhydryl-substituted diiminoacenaphthene-nickel pre-catalysts, **19-22** [75-77]

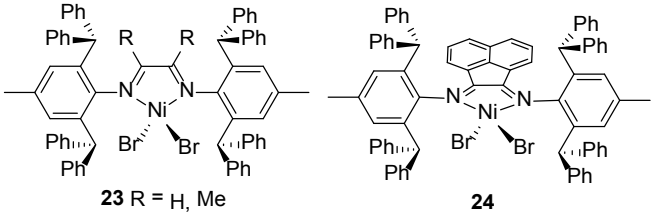

Fig. 9. 2,6-Dibenzhydryl-substituted α-diimine-nickel pre-catalysts, **23** and **24** [78, 79]

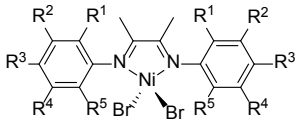

Fig. 10. Fluoro- and trifluoromethyl-substituted α-diimine-nickel pre-catalysts, **25** [80]

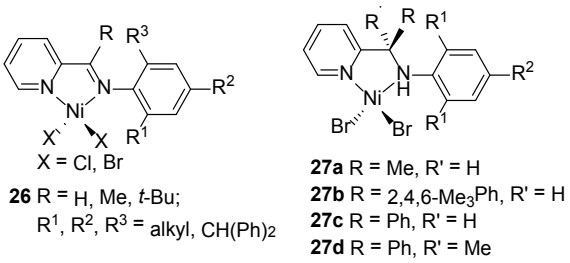

Fig. 11. Pyridinyl-imine and -amine pre-catalysts, **26** and **27** [81-84]

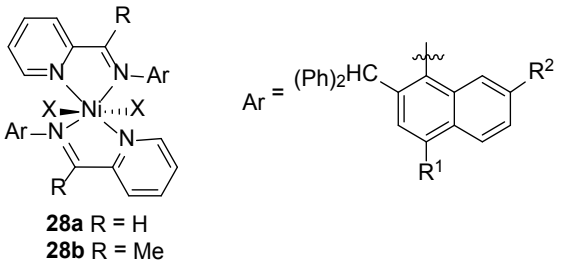

Fig. 12. Sterically bulky N-naphthyl-containing pyridinylimine-nickel pre-catalysts, **28**

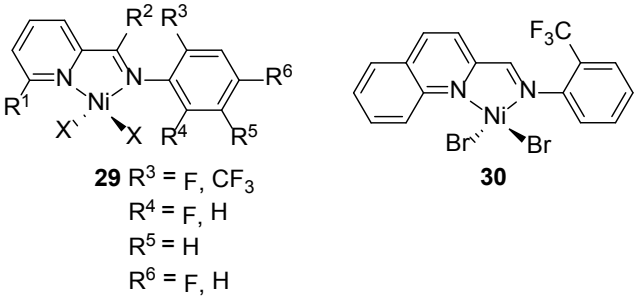

Fig. 13. CF_3- and F-substituted pyridinylimine-nickel pre-catalysts, **29** and **30** [87]

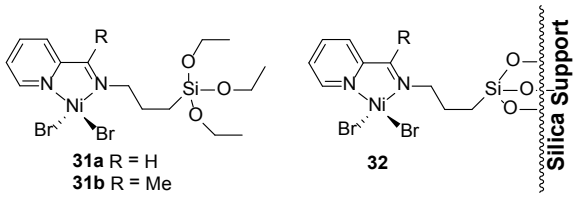

Fig. 14. Alkoxysilyl-containing pyridinylimine-nickel pre-catalysts, **31** and **32** [88]

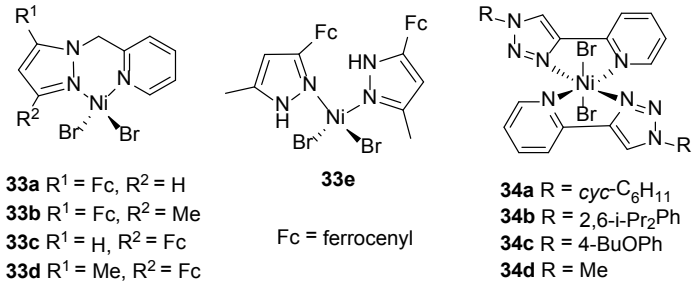

Fig. 15. Pridinylpyrazolyl- and pyridinyltriazole-nickel pre-catalysts, **33** [89] and **34** [42]

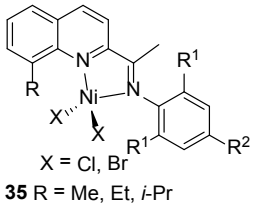

Fig. 16. Quinolinylimine pre-catalysts, **35** [90-91]

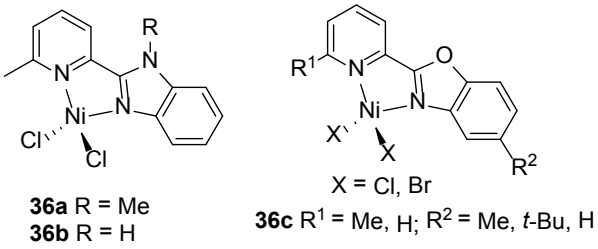

Fig. 17. Pyridinylbenzimidazole- and pyridinylbenzoxazole-nickel pre-catalysts, **36** [92, 93]

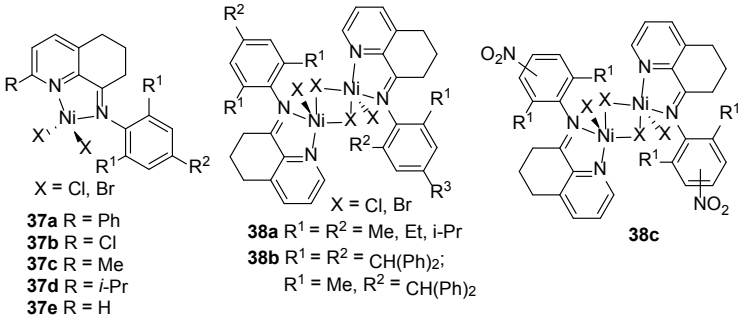

Fig. 18. 8-Arylimino-5,6,7-tetrahydroquinoline-nickel pre-catalysts, **37** and **38** [94-101]

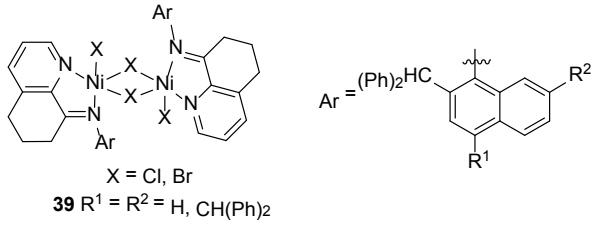

Fig. 19. Benzhydryl-substituted 8-naphthylimino-5,6,7-tetrahydroquinoline pre-catalyst, **39** [103]

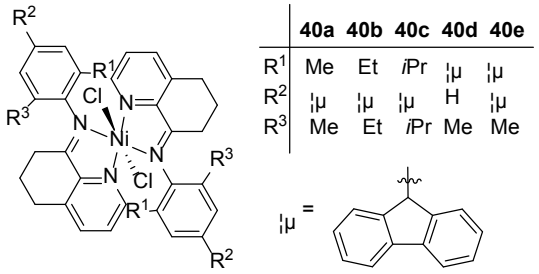

Fig. 20. Fluorenyl-substituted 8-arylimino-5,6,7-tetrahydroquinoline pre-catalysts, **40** [104]

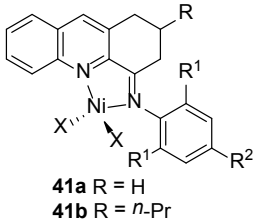

Fig. 21. 4-Arylimino-1,2,3-trihydroacridyl-nickel pre-catalysts, **41** [105,106]

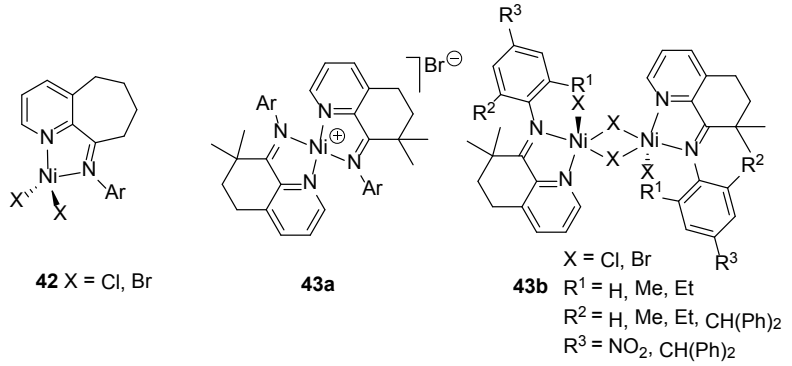

Fig. 22. Iminocyclohepta- and iminocyclohexa-pyridine-nickel pre-catalysts, **42**, **43a** and **43b** [107-110]

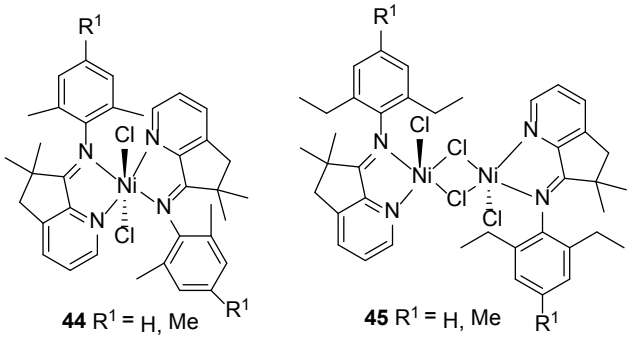

Fig. 23. Imino-cyclopenta[b]pyridine-nickel pre-catalysts, **44** and **45** [111]

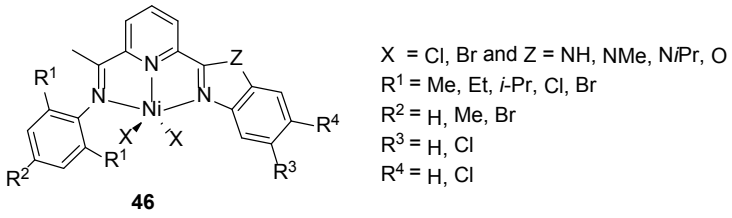

Fig. 24. 2-Imino-6-benzimidazolyl/benzoxazolyl-pyridine-nickel pre-catalysts, **46** [92, 112-115]

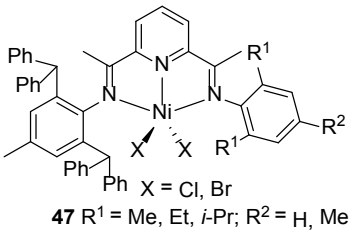

Fig. 25. Unsymmetrical bis(imino)pyridine-nickel pre-catalysts, **47** [116]

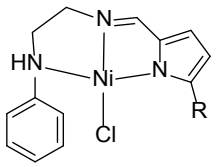

48a R = H
48b R = *t*-Bu

Fig. 26. Pyrrolide-imine-amine-nickel pre-catalysts, **48** [117]

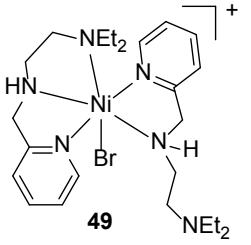

49

Fig. 27. Cationic pyridinylaminoamine-nickel pre-catalyst, **49** [118]

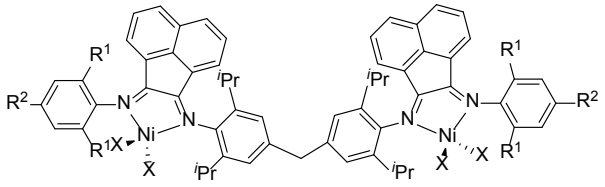

50a R^1 = Me, R^2 = H, X = Br
50b R^1 = Et, R^2 = H, X = Br
50c R^1 = i-Pr, R^2 = H, X = Br
50d R^1 = Me, R^2 = Me, X = Br
50e R^1 = Et, R^2 = Me, X = Br
50f R^1 = Me, R^2 = Me, X = Cl

Fig. 28. Methylene-bridged dinickel bis(α-diimine) pre-catalysts, **50a-f** [71]

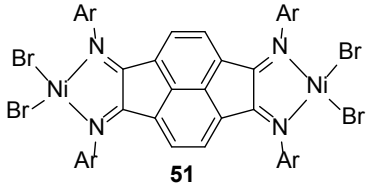

51

51a Ar=2,6-$(Me)_2C_6H_3$
51b Ar=2,6-$(i\text{-}Pr)_2C_6H_3$

Fig. 29. Bis(α-diimine) dinuclear nickel pre-catalysts, **51a** and **51b** [119]

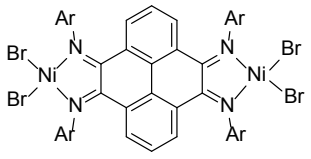

52

52a Ar=2,6-$(Me)_2C_6H_3$
52b Ar=2,4,6-$(Me)_3C_6H_2$

Fig. 30. Pyrenylidene-bridged bis(α-diimine)-dinickel pre-catalysts, **52a** and **52b** [120]

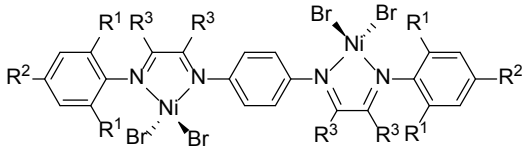

53a $R^1 = R^2 = R^3 = Me$; **53b** R^1 = *i*-Pr, R^2 = H, R^3 = Me;
53c $R^1 = R^2 = Me$, $R^3 = C_{10}H_6$; **53d** R^1 = *i*-Pr, R^2 = H, $R^3 = C_{10}H_6$

Fig. 31. Aryl-linked bis(α-diimine)-dinickel pre-catalysts, **53a-d** [121]

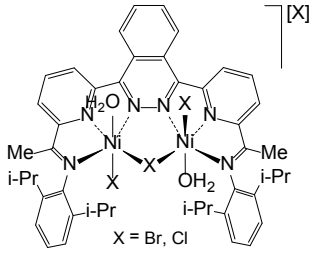

54

Fig. 32. Bis(iminopyridyl)phthalazine-dinickel pre-catalysts, **54** [122]

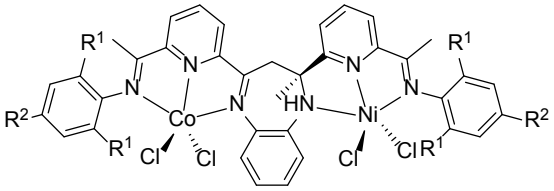

55a $R^1 = Me$, R^2 = H; **55d** $R^1 = Me$, $R^2 = Me$;
55b $R^1 = Et$, $R^2 = H$; **55e** $R^1 = Et$, $R^2 = Me$
55c R^1 = *i*-Pr, $R^2 = H$;

Fig. 33. Heteronuclear Ni-Co pre-catalysts, **55a-e** [123]

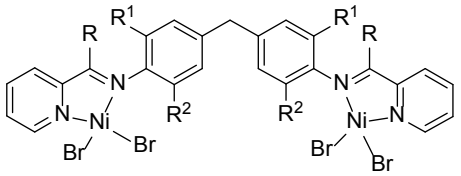

56a R = H, $R^1 = R^2$ = Me
56b R = H, $R^1 = R^2$ = Et
56c R = H, $R^1 = R^2$ = *i*-Pr
56d R = H, R^1 = *i*-Pr, R^2 = Me
56e R = Ph, $R^1 = R^2$ = Me
56f R = Ph, $R^1 = R^2$ = Et
56g R = Ph, $R^1 = R^2$ = *i*-Pr
56h R = Ph, R^1 = *i*-Pr, R^2 = Me

Fig. 34. Methylene-bridged bis(pyridinyliminonickel) pre-catalysts, **56a-h** [124]